Functionality of ruthenium complex self-assembled multilayer-based junctions at a low (≈5%) and high (≈50%) relative humidity

THESIS

submitted in partial fulfillment of the
requirements for the degree of

BACHELOR OF SCIENCE
in
PHYSICS

Author:	X.G.A. Le Large
Student ID:	s1219324
Supervisor:	Dr. ir. S.J. van der Molen
2nd corrector:	Prof. dr. J.M. van Ruitenbeek

Leiden, The Netherlands, August 17, 2016

Table of contents

Abstract

In the search of small and functional molecular devices, we have created and investigated 20 different self-assembled multilayers (SAMTs) each consisting of two self-assembled monolayers (SAM) on top of each other. We compare the molecular combinations to their inverse combinations, investigate their length dependence on the conductance and look for interesting features. Each SAM consists of one type of molecule (there are five different ruthenium complex molecules in total) and each bilayer is grown on an indium tin oxide substrate. Then current-voltage (I-V) curves are taken using conductive atomic force microscopy (C-AFM) to characterize the samples after the relative humidity (RH) of the setup has been brought to ≈ 5% and ≈ 50% respectively and the rectification ratio (RR) for each molecular combination is calculated. Double layers consisting of the same Ru-complexes and combinations of different molecules are measured. We find that while the shape of the I-V curves and the conductance of the combinations are different compared to those of their inverse combination, the rectification ratio (RR) (and in particular the direction of rectification) is not. The highest RR found is $RR_{humid} = 10^{-2.0\pm0.6}$ at 1.0 V for the combination with bottom layer 1-Ru-N and top layer 2-Ru-N (decoupled). Furthermore, we see that while most bilayers have current values that agree to a conductance that decreases exponentially with the length, some do not. Lastly, we observe hysteresis in three samples. Our findings in this exploratory experiment contribute to the knowledge of charge transport in junctions consisting of layers of complex molecules.

1. Introduction

In molecular electronics, it has always been a goal to replace circuit components with integrated molecular junctions to reduce the size of that particular device. The first single-molecule diode, based on the p-n junction in semiconductor physics, was proposed in 1974[1], meaning that if a full-scale electronic circuit can be build out of such molecules, the size would be reduced from several microns to a few nanometers. A lot of challenges had to be overcome, such as contacting the molecules, and it would take until 2005 before the first single-molecule diode was realized[2]. Furthermore, molecules have the advantage that they can provide additional functionalities using synthetic chemistry, in contrast to semiconductor devices. Nowadays, it is more likely that molecular junctions will be used to complement the silicon based electronics with additional functionalities rather than replace them. There are still many problems that have to be solved before one can create molecular devices[3].

Aside from the practical motivation, the research in this field has raised many fundamental questions, for example about the effect of the chemical structure of molecules at their conductive properties. The numerous studies that have been performed at the single-molecule level have greatly increased the understanding of different aspects of mesoscopic charge transport phenomena, the physics that serves as a bridge between the macroscopic world of the bulk materials (the leads) and the microscopic world of atoms (the molecular junctions)[4,5].

1.1 Rectification ratio and single-level model

A single-molecule diode is a molecule that exhibits the same characteristics as its macroscopic counterpart, i.e. it conducts primarily in one direction. The quantity that describes this diode behavior is called the rectification ratio (RR), the current ratio of forward and reverse bias:

$$RR = \left|\frac{I(V)}{I(-V)}\right| \tag{1}$$

For a better understanding of rectification in junctions like the ones in our experiment, we treat the so-called single-level model (often referred to as resonant-tunneling model) in more detail. Conduction takes places through the molecular orbital that is closest to the Fermi energy of the junction, being either the *highest occupied molecular orbital* (HOMO), or the *lowest unoccupied molecular orbital* (LUMO)[4]. These molecular energy levels are depicted as an example in fig. 1 on the next page.

A Landauer-like expression for the current in a metal-molecule-metal (MMM) junction through which we assume phase-coherent off-resonant tunneling at zero temperature is

$$I = \frac{2e}{h}\int_{-eV/2}^{eV/2} T(E,\varepsilon,\Gamma)\,dE \tag{2}$$

where *e* is the fundamental unit of charge, *h* Planck's constant, *V* the applied bias voltage and $T(E,\varepsilon,\Gamma)$ the energy-dependent transmission function. For a single-level, this Lorentzian peaked transmission function is given by

$$T(E,\varepsilon,\Gamma) = \frac{(\Gamma/4)^2}{(E-\varepsilon)^2+(\Gamma/4)^2} \tag{3}$$

where Γ is the (level) broadening, which is proportional to the strength of the coupling to the contacts[6], E the energy and ε the molecular level energy.

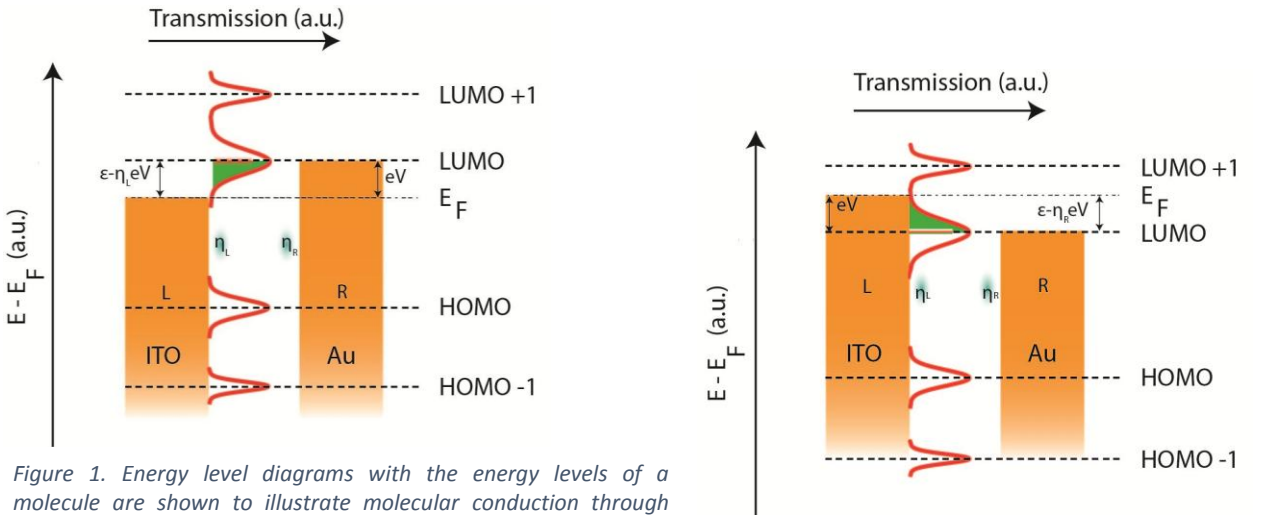

*Figure 1. Energy level diagrams with the energy levels of a molecule are shown to illustrate molecular conduction through tunneling. Each molecular energy level has a Lorentzian-shaped transmission function centered at it. When no bias voltage is applied, the chemical potentials of the left (L, here the indium tin oxide substrate) and right lead (R, here the AFM tip coated with gold) are both at the Fermi level with energy E_F. When a bias voltage is applied, the chemical potentials shift so that they are not on the same level, which results in a current flow. The molecular levels move along with the bias voltage. The part of the transmission function of the molecular energy level that is closest to the Fermi level of the electrodes (in both situations the LUMO) that falls in the bias window (shaded green) is proportional to the current. The voltage drop between the molecule and the left electrode (η_L) and between the molecule and the right electrode (η_R) are in this example equal ($\eta_L = \eta_R = 0.5$), so that the green-shaded area of resonance that falls in the bias window at a negative bias voltage **(left)** is equal to the area at the same but positive voltage **(right)**. This results in symmetric current-voltage (I-V) characteristics.*

In figure 2, energy level diagrams with the transmission function depicted between two electrodes, namely tip (T) and substrate (S) (fig. 2a), are shown to give an example of a rectification mechanism in this model. In this case, the voltage drop between the molecule and the left electrode is not equal to the voltage drop between the molecule and the right electrode, which results in asymmetric I-V curves. By applying a bias voltage between tip and substrate, their chemical potential both shift relative to the resonance position. Then an area of the resonance falls in the bias window, proportional to the current that flows through the junction (fig. 2b). At the same but reverse bias voltage, the difference between the chemical potentials is also *eV*, but while the molecular resonance is still at ε relative to the substrate chemical potential, it is now at $\varepsilon + eV$ relative to the tip. Integrating over the bias window yields a smaller area of the Lorentzian and thus a lower current (fig. 2c). Comparing these pictures gives an explanation for a possible rectification mechanism in the resonant-tunneling model.

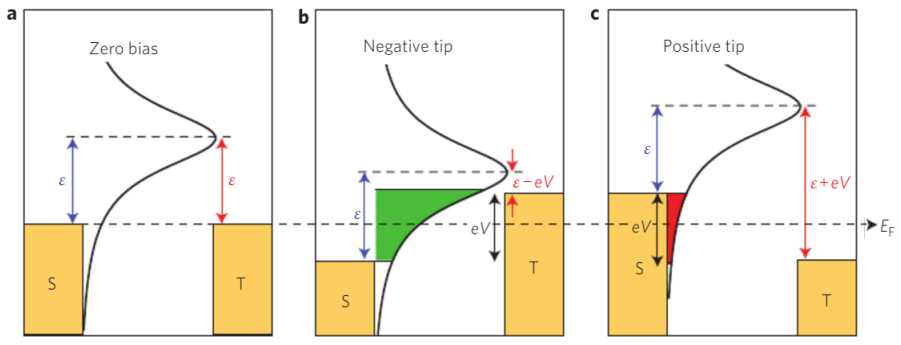

*Figure 2. Picture by Capozzi et al.[7]. Energy level diagrams illustrating a rectification mechanism based on the transmission function. **a**, At zero bias, the molecular resonance has peak energy ε relative to the chemical potentials of both tip (T) and substrate (S) which are at the Fermi levels EF. **b**, With a negatively biased tip, the molecular resonance is at $\varepsilon - eV$ relative to the tip chemical potential and at ε relative to the substrate chemical potential. Increasing the bias voltage has resulted in a bias window with different chemical potential of the leads. The green shaded area of the resonance falls within the bias window, representing a relatively high current. **c**, When the tip is biased positively, the molecular resonance is at $\varepsilon + eV$ relative to the tip and still at ε relative to the substrate chemical potential, but now the bias windows only contains a part of the tail of the Lorentzian, resulting in a relatively small current at the same but reverse voltage.*

While this resonant-tunneling model is helpful in explaining molecular charge transport and rectification, we will not use it in the discussion of the results as our system is more complicated than the single-level case in a self-assembled monolayer (SAM). A two-level system does not apply as well as there are no electronically coupled localized molecular orbitals (LMO's) (which is so in the case of a SAM consisting of 2-Ru-N molecules[8]). Currently, a suitable model is being developed.

1.2 Chemical structure of the used molecules

The molecules that we use for this experiment are called ruthenium complex molecules (see Appendix A) and they are synthesized for conductive as well as optical experiments. Their chemical structure completely determines how they behave as elements in an electronic circuit. For instance, the anchoring groups, that bind the molecule to the (metal) electrodes or just to the substrate, influence the conductance of the junction by controlling the position of the relevant molecular energy levels as well as the strength of the metal-molecule coupling[9]. In our case these terminal groups are tetrapodal phosphonic acid groups. They are located on both sides of the molecules, except for 1-Ru-Py, which has one tetrapodal phosphonic acid anchoring group on one side but a pyridine ring on the other side. The latter is also an anchoring group, but the $ZrCl_2O$ ions (which are also present) do not bind to these pyridine anchoring group which makes a SAM consisting of 1-Ru-Py a termination layer. In practice, this means that it is possible to create self-assembled multilayers (SAMTs) with all Ru-complex molecules as bottom molecule except for the 1-Ru-Py molecule. When creating bilayers, this results in a total of 20 combinations instead of the mathematical total of 25. The theoretical length of the molecules are given in table 4 in Appendix B.

Furthermore, to counter the charge of the molecules, the Ru-complex solutions each contain large mobile PF_6^- anions as counter-ions (see fig. 25 in Appendix A) of which their presence is not a factor of importance in the conductance mechanism[10]. Lastly, $ZrCl_2O$ ions (with molecular length 160 pm) are used to act as buffer layer between two SAMTs. Because of their small length compared to that of the bilayers, which have lengths between 2.4 nm and 6.2 nm, we will neglect their part in the length dependence of the conductance (sections 3.3 - 3.8). This buffer layer holds the molecular layers together by strong zirconium phosphonate groups [19]. However, its effect on the conductance of the molecular combination is not known. We have assumed that its presence does not affect the I-V characteristics of the measured sample as much as the molecules of which the SAMTs exist, but to reveal its exact role, further research is needed.

1.3 Length dependence of resistance and barrier height

Molecular junctions with charge transport (mainly) in the tunneling regime have a resistance that increases exponentially with their length. According to the expression for the current in the Simmons model, at low bias (< 100 mV) the equation for the resistance is given by

$$R(d) = R_0 exp\,(\beta d) \tag{4}$$

where R_0 is the contact resistance, β the tunneling decay constant (with units of inverse length) and d the molecular length[11]. In this model, the expression for β is

$$\beta = \frac{2\sqrt{2m\varphi}}{\hbar} \tag{5}$$

where m is the electron effective mass, $\hbar$ the reduced Planck constant and φ the potential barrier height, which corresponds to the difference between the energy of the Fermi level and that of the nearest molecular orbital through which conduction takes place. This barrier height is different for each molecule. Combined with the facts that the current does not increase linearly with the voltage at a higher bias voltage and that it is not self-evident that the difference between molecular energy levels is

the same, it is not likely that equation 4 is applicable to inhomogeneous bilayers. We will still use this length dependent relation for the conductance (the inverse of resistance) at -1.0 V in sections 3.3 - 3.8 to compare the current levels of different combinations with each other while looking at their molecular length.

Typical values for β vary from 2-6 nm^{-1} for π-conjugated molecules and 9 nm^{-1} for alkanethiol molecules[12], and depends in general on the nature of bonding in the molecular backbone. The attenuation factor is reported to be lower for a series of ruthenium redox-active conjugated molecular wires (β =0.9 nm^{-1}), showing a very weak length dependence[13]. This could be relevant since we use such organometallic complexes.

1.4 Humidity dependent measurements

Recently it has been found that a SAM consisting of 2-Ru-N molecules (see Appendix A) has a switchable diode behavior[8], i.e. it behaves as a (strong) diode when the relative humidity is changed from ≈ 5% to ≈ 50%. The RR increases from nearly unity to $10^{3.1\pm0.6}$ (at 0.9 V) respectively, as can be seen in figure 3. This is the highest rectification ratio reported yet and special in the sense that its switchable behavior could be of interest when applied to the design of switchable molecular devices, such as nanoscale sensors.

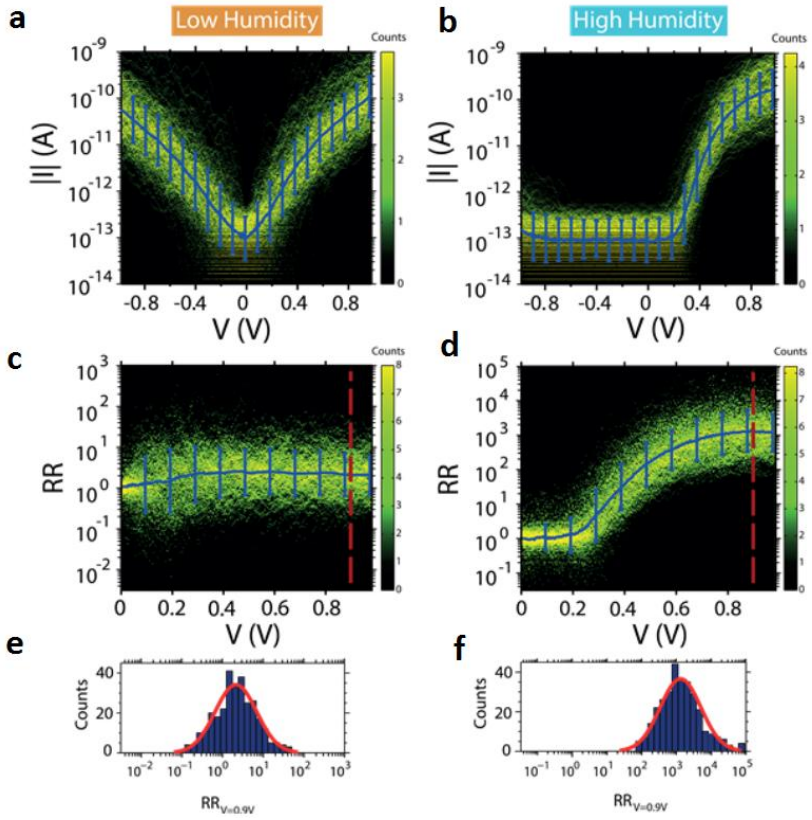

Figure 3. 2D-histograms containing data from measurements done by H. Atesci, V. Kaliginedi et al.[8]. In fig. 2a and fig. 2b, the absolute value of the measured current is plotted against the bias voltage as a semi-log plot in a bias window ranging from -1.0 V to 1.0 V. In fig. 2c and fig. 2d, the RR is calculated for each bias voltage as done in eq. 1 and also plotted as a semi-log plot. The red-dotted lines indicate the voltage at which the RR is maximum. The error bars come from the half widths of the fits. ***a****, At dry conditions (RH ~ 5%), the IV-curve is symmetric.* ***b****, At a RH of about 50%, the IV-curve clearly becomes asymmetric, meaning that the current flows mainly in one direction.* ***c****, The corresponding plot of the rectification ratio in the dry case is near unity for almost every bias voltage, as follows from the given definition.* ***d****, At a high RH the corresponding RR equals $10^{3.1\pm0.6}$ at 0.9 V.* ***e****, The intersection of the data in the 2D log(RR)-V histogram at 0.9 V is displayed and fit as a Gaussian at a low RH. In* ***f****, The same is done at a high RH.*

1.5 Description of the project

In this bachelor research project, we continue the exploration of the humidity dependent conductance and to this end we use the five different Ru-complex molecules to create 20 different bilayers. We investigate their current-voltage (I-V) characteristics and try to relate their chemical structure and theoretical length to their conduction properties. It is based on the research conducted by H. Atesci, V. Kaliginedi et al.[8] and in the same way is the relative humidity changed and are the measurements done and analyzed.

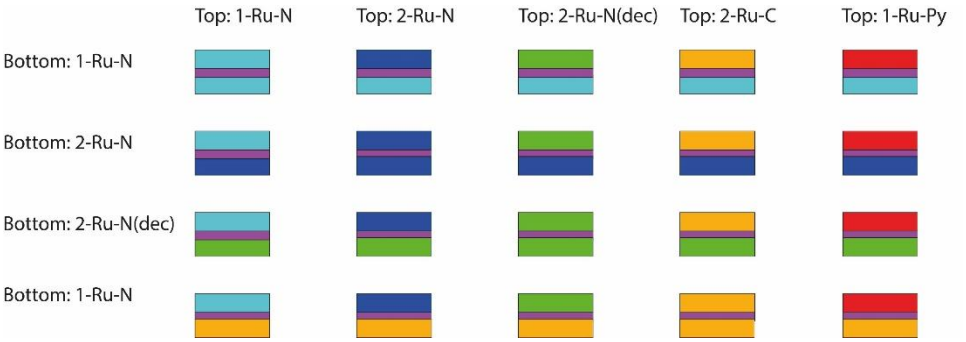

Figure 4. Schematic overview of the 20 possible combinations of bilayers that are all created and measured. Light blue: 1-Ru-N, dark blue: 2-Ru-N, green: 2-Ru-N (decoupled), yellow: 1-Ru-N and in purple the buffer layer between two SAM's.

The research questions are as follows:

1. How do the double layers and monolayers that both consist of the same molecules compare to each other? In other words, are the shapes of their I-V curves and their rectifying behavior the same or completely different?
2. Do bilayers with the same bottom or top molecular layer have features in common?
3. How do the molecular combinations compare to their inverse combinations? In other words, are the shapes of their I-V curves and their rectifying behavior the same or completely different?

While it is difficult to make an educated guess about the results in this exploratory experiment, we can still try to do this, so that we can compare the results with this. For the double layers (the bilayers that consist of the same molecule, shown in the diagonal of fig.4), we expect a resemblance to the monolayers that also consist of that particular molecule regarding the shape of their I-V characteristics. For the other combinations, we expect I-V curves that look like the average of those of the SAM's of which they consist, but completely different shapes are also possible. Regarding their total length, both types of bilayers are expected to have lower current values than the SAMs. Furthermore, we expect that the current values of the bilayers are comparable to their inverse combinations. Finally, we cannot make a prediction about the (a)symmetric shape of the combinations yet, so also not about the value of the RR. However, we expect a different shape of the I-V curves when the RH is increased, as is the case for the SAMs consisting of the same molecules[8].

In summary, the project goals are to create the bilayers, measure the current through the molecular junctions in the dry case as well as in the humid case, calculate and plot their rectification ratios, compare the I-V curves by doing a quantitative analysis and to look for an explanation for the (possibly unexpected) results.

2. Methods

2.1 Sample fabrication

The setup of the experiment is as follows. First, the substrate, indium tin oxide (ITO) coated glass, is cut so that its size is about 0.5 by 0.5 cm. Then we use two methods to clean it. For the first one we put it in RCA Standard Clean-1 for one hour. This is prepared by making a solution of five parts of deionized water, one part of aqueous ammonia (25% NH_3 in H_2O) and one part of hydrogen peroxide (H_2O_2 (l)), after which the solution is heated to 80°C for one hour. When there are no bubbles around the substrate anymore, the reaction is over and organic contaminants are removed. Then we take the substrate out of the solution, rinse it with copious amounts of purified water (≈ 1L Milli-Q water) and then gently blow it dry with nitrogen gas (N_2 (g)) so that there are no residues of the RCA solution. The next cleaning method is optional, but always used for the samples in this experiments. The sample is etched for 3 minutes with an argon ion beam (350 eV, 10mA) at a pressure of $3x10^{-4}$ mbar. The platinum tip (which has a tip radius < 20nm and is coated with an additional 150 nm of gold) of the conductive atomic force microscope (C-AFM) is also etched, but only for 10 seconds. Meanwhile, we grow a self-assembled monolayer of ruthenium complex molecules on the ITO side of the etched substrate. This can be achieved by putting the substrate in the solution of the ruthenium complex molecules. The phosphonic acid groups are adsorbed onto the ITO, after which the molecules self-assemble in an organized pattern. The molecular density on the surface increases so that a SAM is formed.

After one hour, we take the substrate out of the solution, rinse it again with the purified water so that only the first layer of molecules (that is covalently bound) remains attached and then again blow it dry with the nitrogen gas. For a monolayer, we now put the substrate in the AFM. For self-assembled multilayers (SAMTs), we grow a buffer layer consisting of an aqueous solution of $ZrCl_2O.8H_2O$ on each ruthenium complex layer, by laying the sample in the buffer solution for half an hour. The solution is made by dissolving $ZrCl_2O$ powder into water until it has a molar concentration of 1 mM. To prevent polymerization it is essential to rinse the tweezers each time. By repeating this process, it is possible to grow numerous ruthenium complex layers on the substrate, each separated by a buffer layer (see figure 5).

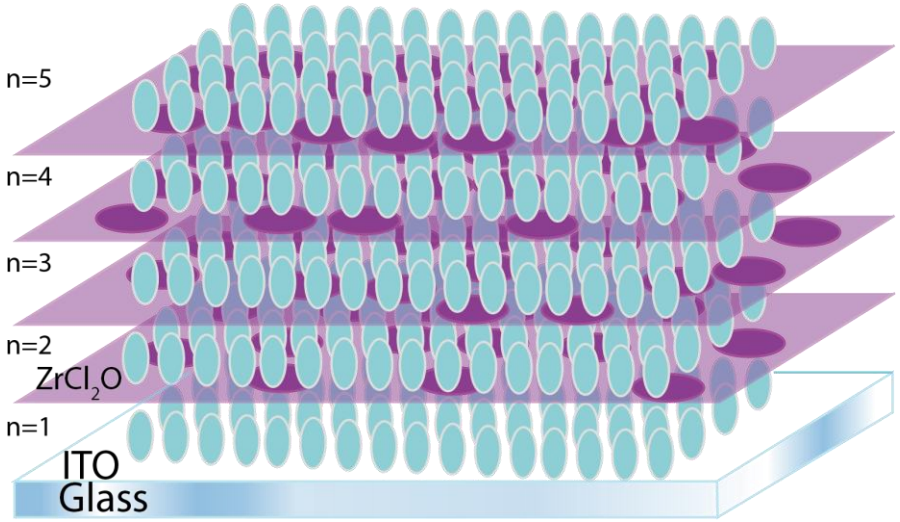

Figure 5. Multilayers of 1-Ru-N molecules (light blue) and $ZrCl_2O$ buffer layers (purple) on an indium tin oxide substrate. We assume that the SAMTs are well ordered molecular assemblies and that the buffer layer has a negligible thickness compared to that of the Ru complex molecules.

2.2 Experimental setup

After the preparation of the SAMTs, we characterize the sample using C-AFM (see figure 6[a]). A sharp tip at the end of a conductive cantilever approaches the surface of the sample. The deflection of this cantilever, which is caused by the attractive Van der Waals force at close-range and the repulsive interatomic interactions between surface and tip when contact is made, is read out using a focused laser beam and a position-sensitive photodiode. The height of the tip is controlled by a piezoelectric element in a feedback loop in order to keep the deflection voltage constant and to ensure a stable contact between tip and sample at a force setpoint of 10.5 nN. By applying a bias voltage between tip and sample (the bias is applied to the sample and the tip is grounded), a current flows through the ruthenium complex molecules (see figure 7). Roughly ~100 molecules are probed, this varies from junction to junction. The current-voltage curves that are obtained provide information on the differential conductance and (eventual) diode behavior of the multilayers.

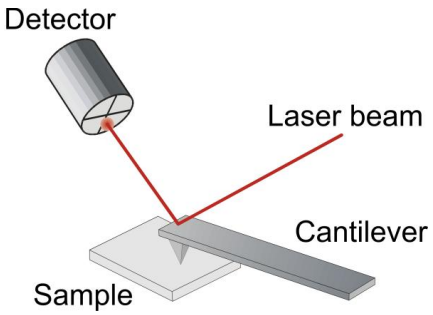

Figure 6. When the cantilever is deflected due to interactions between tip and sample, the laser beam reflects on a different spot on the photodiode, thereby changing the reflection voltage.

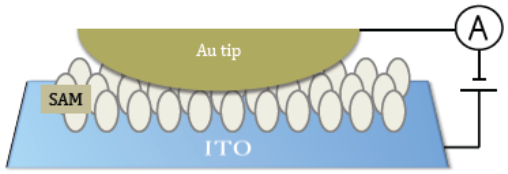

Figure 7. A schematic overview of the atomic force microscopy setup. A bias voltage is applied between the AFM tip and the sample so that a current flows through the molecules. An I/V converter is also used, after which the signal is registered with a PC that takes IV-curves.

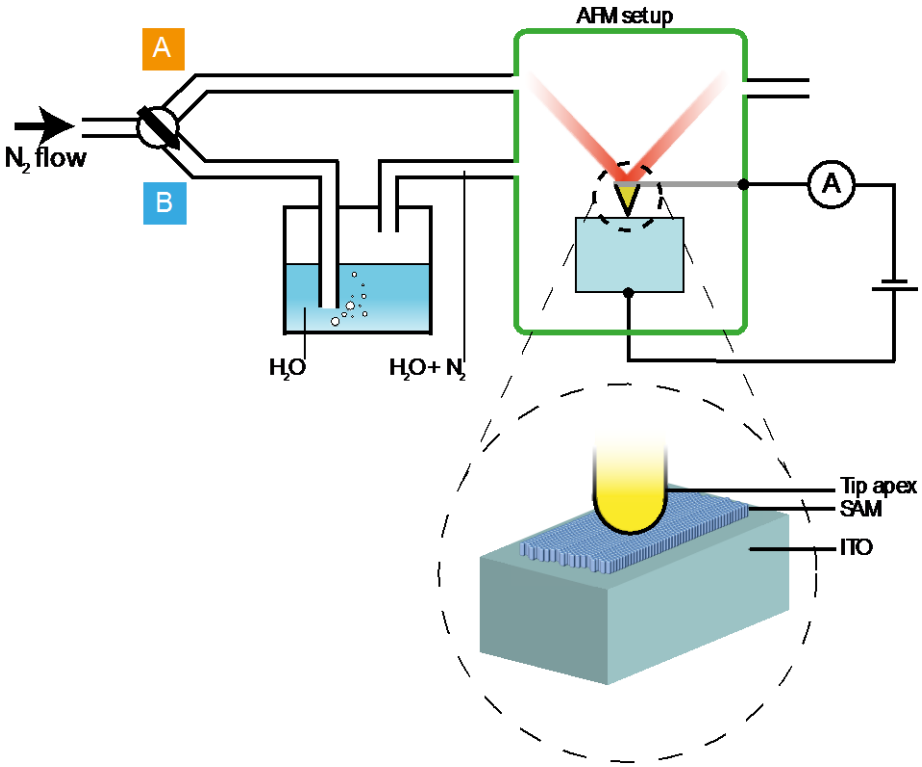

To control the relative humidity (RH), we put a plastic bag over the AFM setup through which we put three tubes (see figure 8). One of them transports nitrogen gas to purge the air and bring it to a RH of ≈ 5%, while the other two can blow nitrogen gas through a beaker filled with heated water in order to increase the RH to ≈ 50% (a higher RH could damage the AFM). In that way, the rectification ratio as a function of the RH can be calculated.

Figure 8. Schematic overview of the experimental setup (picture by Ateşçi, H., Kaliginedi, V. et al.[8]. By letting nitrogen gas flow to the AFM setup or via a beaker of heated water to the AFM setup, the relative humidity can be changed.

2.3 Noise features and current sensitivity

We use a grounded Faraday cage during all measurements to reduce electrical noise, mainly 50 Hz noise. When these unwanted fluctuations, coming from capacitive coupling of the power line, are not filtered out, sinusoidal noise can be seen in the I-V curves (see for example fig. 9a on page 13, where this noise was not filtered out).

Another noise feature in this experiment is the noise floor, which is the current level that separates the region with data points from the region where noise dominates. In order to get I-V characteristics that contain enough information about the molecular junction and to be able to calculate a rectification ratio that has a low upper limit (i.e. the error due to the noise floor is minimized), it is essential to measure a signal that is higher than the noise floor at a part of the bias window that is as great as possible. Thermal noise due to irregular movements of the charge carriers in the molecular junctions are the major source of this noise floor. It could be reduced by lowering the temperature of the setup, which we have not done.

However, adjusting the current sensitivity using the computer software (NanoScope Analysis) can also reduce the noise floor. The highest current sensitivity (20 pA/V with a low bandwidth filter) enables us to detect signals with a current as low as a few hundred fA ($\sim 5 \times 10^{-14}$ A). Lower current sensitivities (100 pA/V and 1 nA/V) are used for higher current values (ranging from 200 pA to 5 nA), because a current sensitivity that is too high would result in a saturated current values at bias voltages where the current is high. When the current sensitivity has been set too low, the noise then dominates at low current values and the noise floor covers an important part of the I-V characteristic (see for example the yellow stripes at current levels lower than 10^{-12} A of the double layer 1-Ru-N in Appendix D on page 41). It is up to the experimentalist to decide which current sensitivity fits the experiment best to prevent a high noise floor as well as saturated I-V curves.

3. Results & discussion

Due to the large amount of collected data (see Appendix D), we categorize our results as follows. First of all, we will show and discuss hysteretic effects occurring in the measurements on three samples at a high RH. Then we will show the I-V characteristics of two samples that have the highest RR (compared to other rectification ratios), one allowing current to flow in forward direction and the other in reverse direction. After that, we compare all the results by plotting their current values at a fixed voltage against the theoretical length of the combinations (see table 4 in Appendix B) for the multilayers 1-Ru-N, other monolayers and for bilayers with the same bottom or top molecular layer. By comparing their values and linear fits, we can investigate their dependence on length and humidity and see if there are particular combinations that conduct better than others. We conclude with a comparison of the rectification ratio at 1.0 V of bilayers with the same bottom or top molecular layer and we will compare the RR of combinations with that of their inverse combinations as well in order to look for a pattern.

3.1 I-V curves and RR plots showing hysteresis at a high RH

Three measurements on the bilayers in a humid environment show hysteretic behavior each at a specific bias voltage range. This means that their trace and retrace (forward and backward direction of current) no longer overlap at the same values of the bias voltage that is swept between -1.5 V and 1.5 V. In order to justify that this truly is hysteresis, an intrinsic property of the sample and not an artifact in the measurements, one must regard two criteria.

Firstly, the ramping rate has to be set low enough to prevent capacitive charging. This phenomenon can also cause hysteretic effects (at a bigger bias voltage range) as can only be seen when measuring molecular junctions when the ramping rate has been set too high, but it is not the one presented here. In all our measurements the ramping rates have values between 0.10 Hz and 0.30 Hz, depending on the conductance of the sample - a higher conductance permits a higher ramping rate.

Secondly, we can only speak of hysteresis if a significant part of the data points does not overlap with the data points that are centered around a different current value at the same voltage. With ‘significant’ we mean that no more than the half width of the error bars of the trace and retrace may overlap. Since they are fit as a Gaussian, the tails of the error bars contain much less data points than their center, so that the presence of two bands is distinct enough. In the following plots the average trace is colored blue and the average retrace is colored red, where average means at the center of the Gaussian fit. The figure axes of these 2D-histograms are comparable to those in fig. 2, except that now the logarithm of the absolute value of the current is displayed on the y-axis (giving for example -12 instead of 10^{-12}) and that the bias window ranges from -1.5 V to 1.5 V in our measurements.

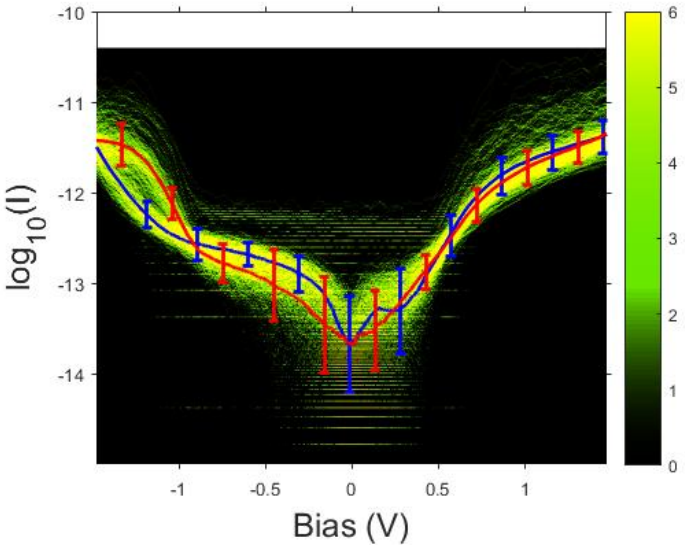

Figure 9a. 2D histogram showing the log|I|-V characteristics of a 2-Ru-N double layer at a high RH. The averaged values of the trace and retrace are colored blue and red respectively. At There is hysteresis between -1.3 V and -1.1 V.

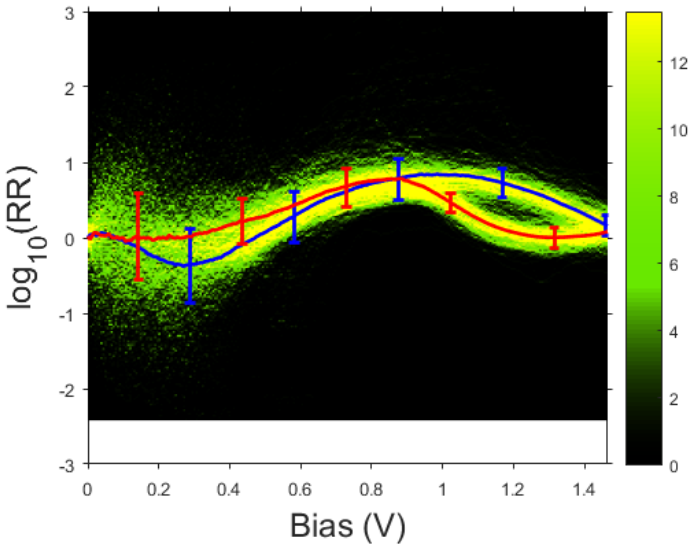

Figure 9b. 2D histogram of the calculated RR of the same combination and RH as in fig. 7a. The averaged values of the trace and retrace are again colored blue and red respectively. This plot also shows the two separate bands in the same range, a sign of hysteresis.

The double layer consisting of 2-Ru-N molecules shows hysteresis between -1.3 V and -1.1 V, where the current values are separated with a factor of $10^{0.5 \pm 0.2}$ (see figure 9a). In figure 9b, the rectification ratio is calculated and shown. Again there are two bands in the same voltage range, since the current ratio at the positive and equal but negative voltage now has two values for one bias voltage.

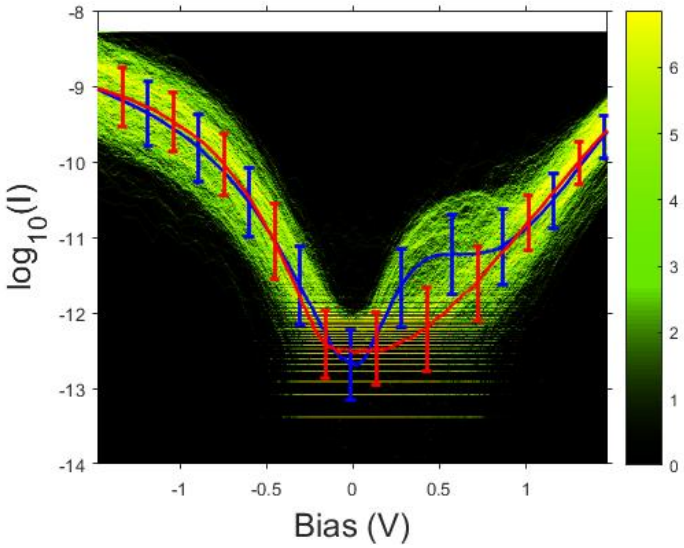

Figure 10a. 2D histogram showing the log|I|-V characteristics of a bilayer with bottom 2-Ru-N(dec) and top 1-Ru-N at a high RH. The averaged values of the trace and retrace are colored blue and red respectively. There is hysteresis between 0.4 V and 0.7 V.

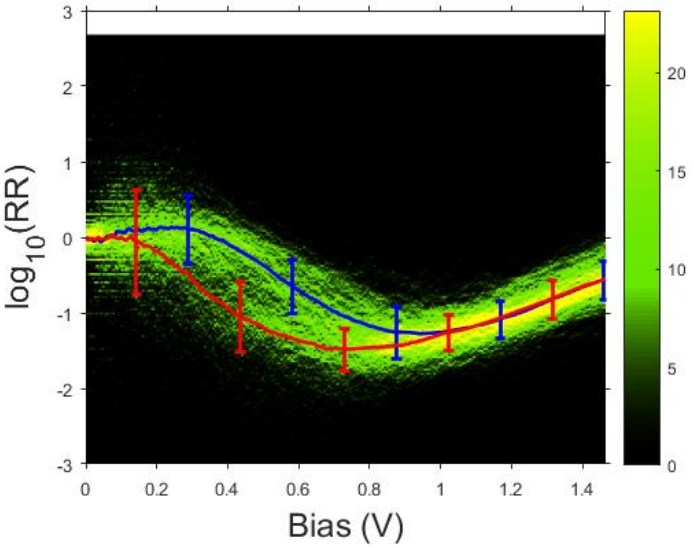

Figure 10b. 2D histogram of the calculated RR of the same combination and RH as in fig. 8a. The averaged values of the trace and retrace are again colored blue and red respectively.

A bilayer with two other molecules, namely bottom molecule 2-Ru-N(dec)[1] and top molecule 1-Ru-N, also contains a region in which there seems to be hysteretic behavior (see figure 10a). From 0.4 V to 0.7 V the error bars overlap each other for maximum 50%. Besides, the averaged values of the retrace clearly follow a different path than those of the trace. The rectification curves confirms this on the same range (see figure 10b).

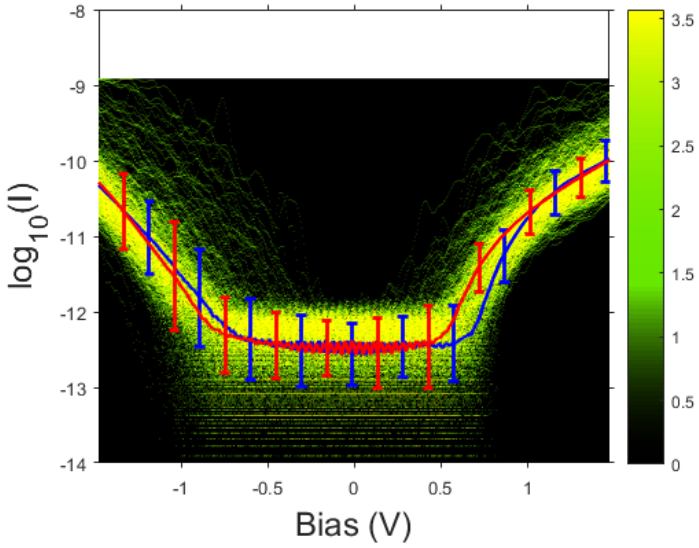

Figure 11a. 2D histogram showing the log|I|-V characteristics of a bilayer with bottom 2-Ru-N(dec) and top 2-Ru-N at a high RH. The averaged values of the trace and retrace are colored blue and red respectively. There is small hysteresis between 0.7 V and 0.8 V. 50 Hz noise is visible between -0.4 V and 0.4 V.

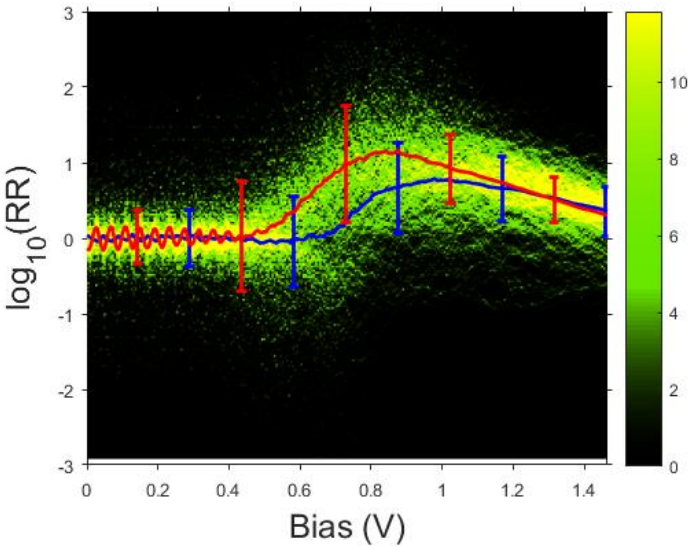

Figure 11b. 2D histogram of the calculated RR of the same combination and RH as in fig. 9a. The averaged values of the trace and retrace are again colored blue and red respectively.

For the last sample where we have encountered hysteretic behavior (with bottom molecule 2-Ru-N(dec) and top molecule (2-Ru-N), we see small hysteresis in a small range around 0.7 V (see figure 11a). By taking a closer look at fig. 11b, we can see that hysteretic effects occur from 0.7 V to 0.8 V.

In measurements done by Lee et al. on a different Ru-complex[14], hysteresis was also observed and compared with a previous experiment where the charging/discharging of the SAM was thought to be the cause, which then acted as a capacitor. However, it is not likely that the observed hysteresis in the measurements on these three samples is caused by capacitive charging, as the sweep rate has been set low enough compared to the measurements on other samples where eventual hysteretic I-V curves disappeared when the sweep rates were set lower (i.e. capacitive charging). Mahapatro et al. also observed hysteresis in the I-V curves of Ru-based redox-active molecules (in MMM nanogap junctions) in slow bias scans and suggested that this is caused by charge storage in the molecules[15]. An experiment conducted by Schwarz et al.[16] indicates an oxidation/reduction mechanism that is mediated by a weakly coupled, localized molecular orbital which also results in functional behavior of hysteresis.

[1] We use 2-Ru-N(dec) as an abbreviation for 2-Ru-N (decoupled).

3.2 Two samples with a high RR and with an opposite direction of rectification

Here we show the I-V characteristics and the corresponding plot of the calculated rectification ratios of two samples. We have chosen to show the ones with the highest RR that we found and each with an opposite direction of rectification. For an overview of the RR at 1.0 V for each combination in the humid case, the reader is referred to table 3.

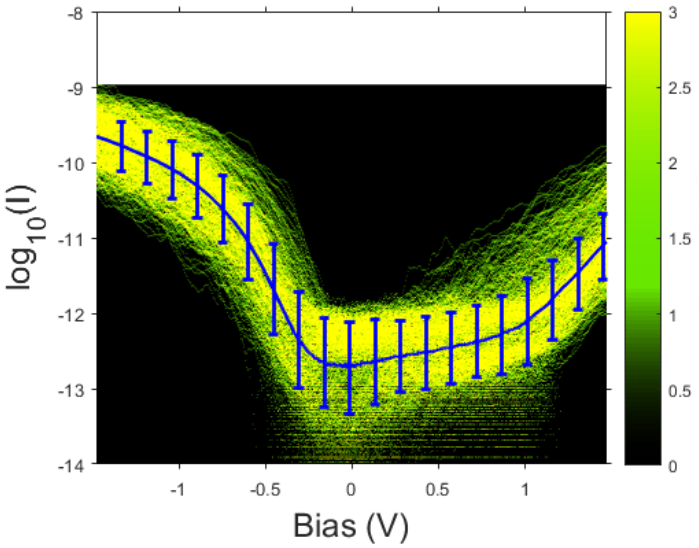

Figure 12a. 2D histogram showing the log|I|-V characteristics of a bilayer with bottom 1-Ru-N and top 2-Ru-N(dec) at a high RH. It is clearly visible that the current values are two orders of magnitude higher at -1.0 V than at 1.0 V.

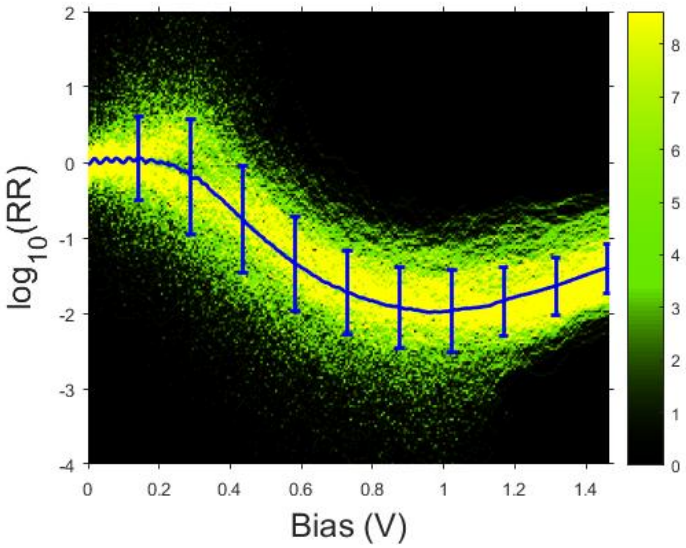

Figure 12b. 2D histogram of the calculated RR of the same combination and RH as in fig. 10a. The rectification is maximum at 1.0 V with $RR_{humid} = 10^{-2.0 \pm 0.55}$.

In fig. 10a and fig. 10b, we see the highest rectification as observed in our measurements on the 20 different bilayers. The sample with bottom layer 1-Ru-N and top layer 2-Ru-N(dec) favors current that flows at a negative applied bias voltage over a positive one. This can especially be seen at the ratio between the current at -1.0 V and at 1.0 V, as the difference is two orders of magnitude there ($RR_{humid} = 10^{-2.0 \pm 0.55}$).

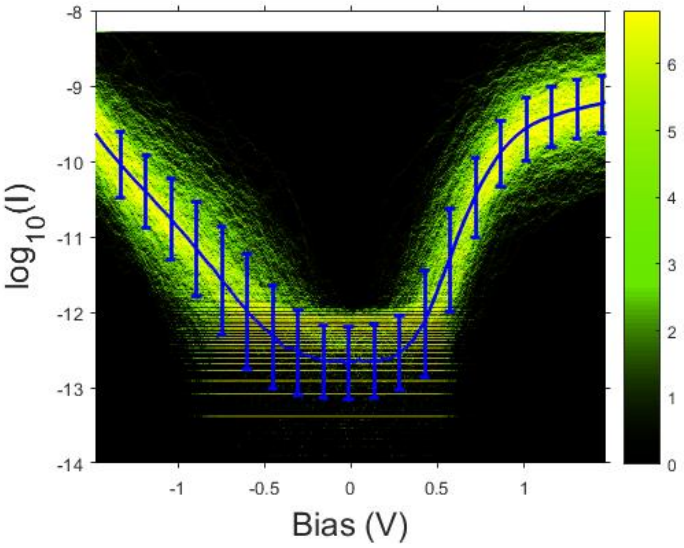

Figure 13a. 2D histogram showing the log|I|-V characteristics of a bilayer with bottom 2-Ru-N and top 2-Ru-C at a high RH.

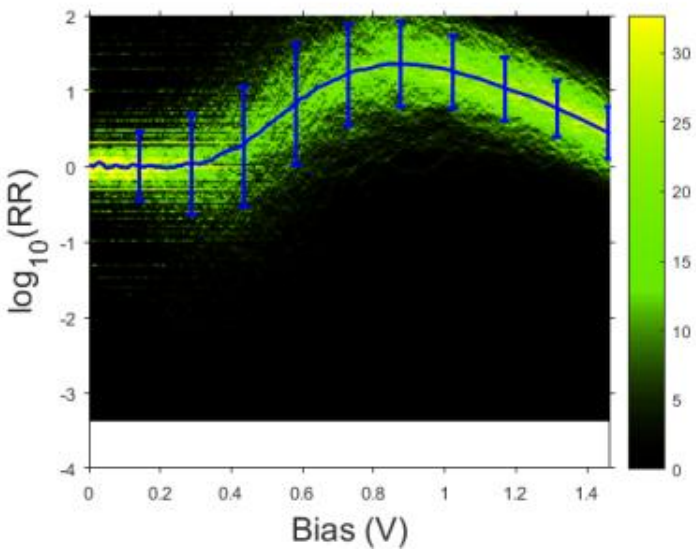

Figure 13b. 2D histogram of the calculated RR of the same combination and RH as in fig. 11a. The rectification is maximum at 0.9 V with $RR_{humid}=10^{1.35\pm0.6}$. Note that this direction of rectification yields a positive value of log(RR).

The other sample, with bottom layer 2-Ru-N and top layer 2-Ru-C, also acts like a diode but with an opposite direction of rectification compared to the previous sample. As can be seen in fig. 11a, the current that flows when a positive bias voltage is applied, is more than one order of magnitude higher than at a negative bias voltage. This is visible in fig. 11b, where $RR_{humid}=10^{1.35\pm0.6}$ at 0.9 V.

3.3 Length and humidity dependence of conductance of SAMTs with bottom 1-Ru-N

In this section, a quantitative analysis of the measurements on the samples is done by plotting the current values at a fixed voltage against the theoretical length of the combinations. The length dependence is investigated by looking at the current values of the molecular combinations at its specific length as well as at the slope of the linear fit, which is the same as the tunneling decay constant β in eq. 4 (section 1.3) but with an opposite sign as we now treat the conductance. We want to point out that in this section and in the next ones, we compare the current values of the bilayers at -1.0 V and generalize the findings to be able to say something about the conductance while not having to compare the current values at all bias voltages. This can be done as the I-V characteristics are symmetric for all samples at a low RH (see Appendix D) and those at a high RH all differ in any case.

It should be noted that not all measurements are done with the same AFM tip, meaning that although the dimensions, material and tip etching steps are the same, the tip apex geometry could vary slightly and so could the current values. However, a comparison between the dry and humid cases can always be done for a particular combination of molecules, as the tip geometry does not change when varying the relative humidity. Furthermore, the reader is referred to Appendix D for the obtained I-V characteristics that give a more complete image of their difference in shape between the dry and humid case, as well as their change in conductance.

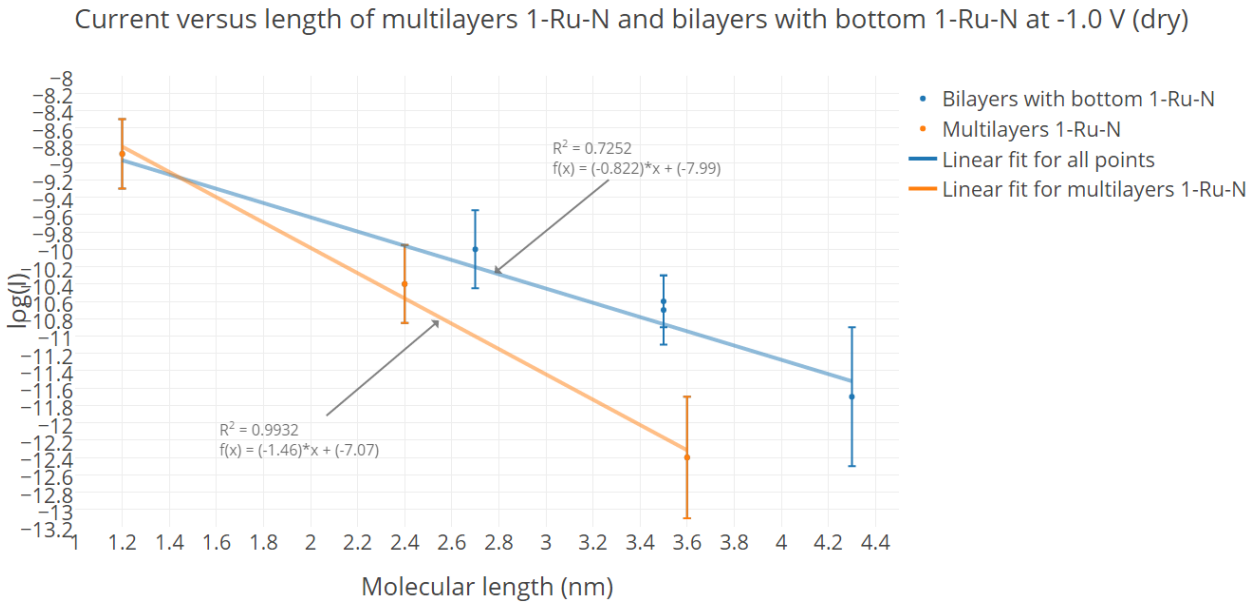

Figure 14. Semi-log plot of the current versus theoretical molecular length of multilayers 1-Ru-N (up to three layers) and bilayers with bottom 1-Ru-N at -1.0 V and at a low RH. The multilayers are colored orange, while the combinations with bottom layer 1-Ru-N are colored blue. The linear fit for the multilayers has a slope of -1.46 ± 0.31 nm-1 and the fit for all data points (multilayers as well as bilayers with bottom 1-Ru-N) has a slope of -0.82 ± 0.21 nm-1. The combination with top molecule 2-Ru-N (at 3.5 nm) has a current value of -10.7 ± 0.4 at this voltage, which lays in the same error range as that of the one with top molecule 2-Ru-C (-10.6 ± 0.3).

For all molecular combination with bottom molecular layer 1-Ru-N in the dry case (see fig. 14), the conductance drops with nearly an order of magnitude per nanometer (-0.8 ± 0.2 nm^{-1}) at that voltage. We take into account that they do not have the same top layer, so the conduction properties are likely to vary from combination to combination. The fact that the fits are linear means that their drop is exponential, as expected according to literature [17]. We see that at 3.5 nm, the combinations with the same length (having top molecules 2-Ru-N and 2-Ru-C) both have almost the same current value, meaning that none of the combinations with bottom molecule conducts better in the dry case.

The multilayers consisting of 1-Ru-N molecules at a low RH also have a conductance that decreases exponentially with the length of the combination. By looking at the slope, we see here that $\beta = 1.5 \pm 0.3$ nm^{-1}.

In fig. 15, the current values of the same combinations as in fig. 14 are plotted against their length, but now at a high RH. First we take a look at the multilayers consisting of 1-Ru-N molecules only. The fit intersects the three data points almost perfectly. Compared to the dry case, the current values seem to be slightly higher, but within the error range.

Next, the only two combinations that have a different conductance are those with top layer 2-Ru-N (at 3.5 nm, lower conductance) and top layer 2-Ru-N (dec) (at 4.3 nm, much higher conductance), which is due to rectification at that voltage. As can be seen in the results for this combination, the rectification ratio for the last one at this voltage is highest of all bilayer combinations. Due to this effect, the current increases from $10^{-1.7\pm0.8}$ A to $10^{-10.2\pm0.4}$ A.

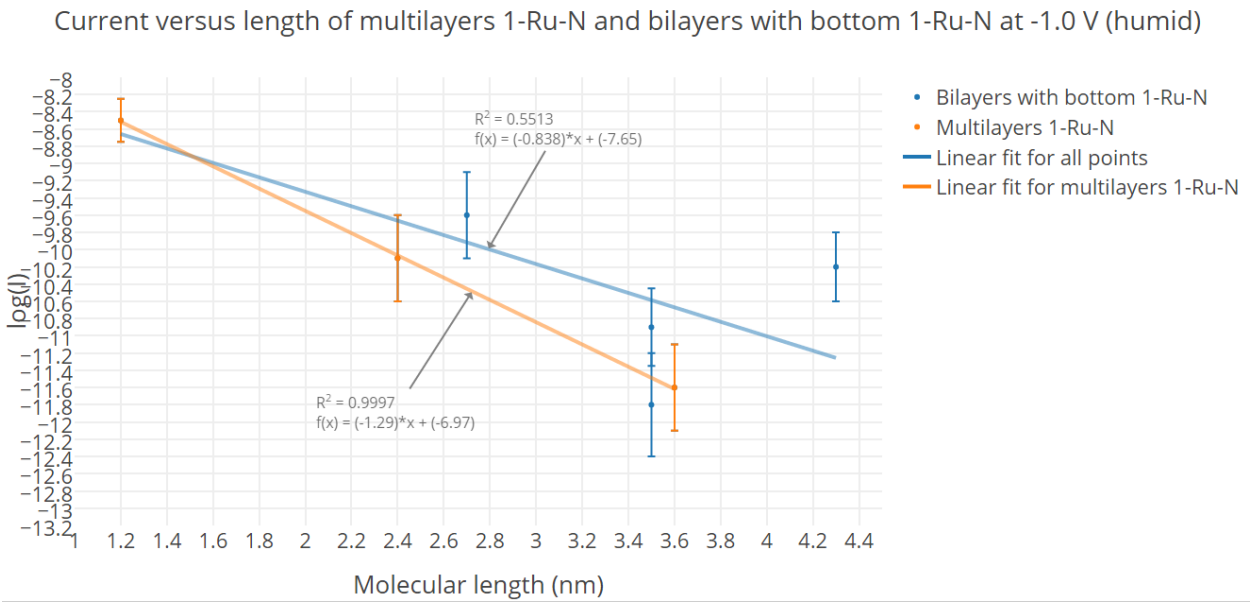

Figure 15. Semi-log plot of the current versus theoretical molecular length of multilayers 1-Ru-N (up to three layers) and bilayers with bottom 1-Ru-N at -1.0 V and at a high RH. The multilayers are colored orange, while the combinations with a different top molecule than 1-Ru-N are colored blue. The linear fit for the multilayers has a slope of -1.3 ± 0.02 nm-1 and the fit for all data points (multilayers as well as bilayers with bottom 1-Ru-N) has a slope of -0.8 ± 0.2 nm-1. The combination with top molecule 2-Ru-N has a current value of -11.8 ± 0.6 which is lower than in the dry case.

3.4 Length and humidity dependence of conductance of bilayers with the same bottom

Now we compare the current values of the bilayers consisting of the same bottom molecule with each other and examine the deviating points (see fig. 16). Again, we begin with the dry case. The data points of the 1-Ru-N mono- and bilayer are obtained from a different measurement, but there are no other differences. A notable feature is the positive slope of the fits for 2-Ru-N and 2-Ru-C. It means that if the data points are averaged, the combination of molecules is a more important factor for the conductance than the length of the bilayer. We see this in particular when comparing the bilayers with bottom 2-Ru-N (marked orange) and top layer 2-Ru-N/2-Ru-C, as the latter has a conductance that is two orders of magnitude higher, while their length is equal. We want to stress that this is the case at a low RH, so there is no rectification effect that could play a role. Furthermore, three out of five bilayers with bottom 2-Ru-C (marked red) have higher current values than bilayers consisting of other bottom layers but equal in length. Finally, the 2-Ru-C double layer and the combination 2-Ru-C with top 2-Ru-N (both again with theoretical length 4.6 nm) have lower current values, the latter being the inverse combination of the bilayer with high conductance. This is one example of the difference in conductance for bilayers with the same Ru complex molecules but grown in different order, the only exception being the combinations of 1-Ru-N with 2-Ru-N (see table 1 on the next page).

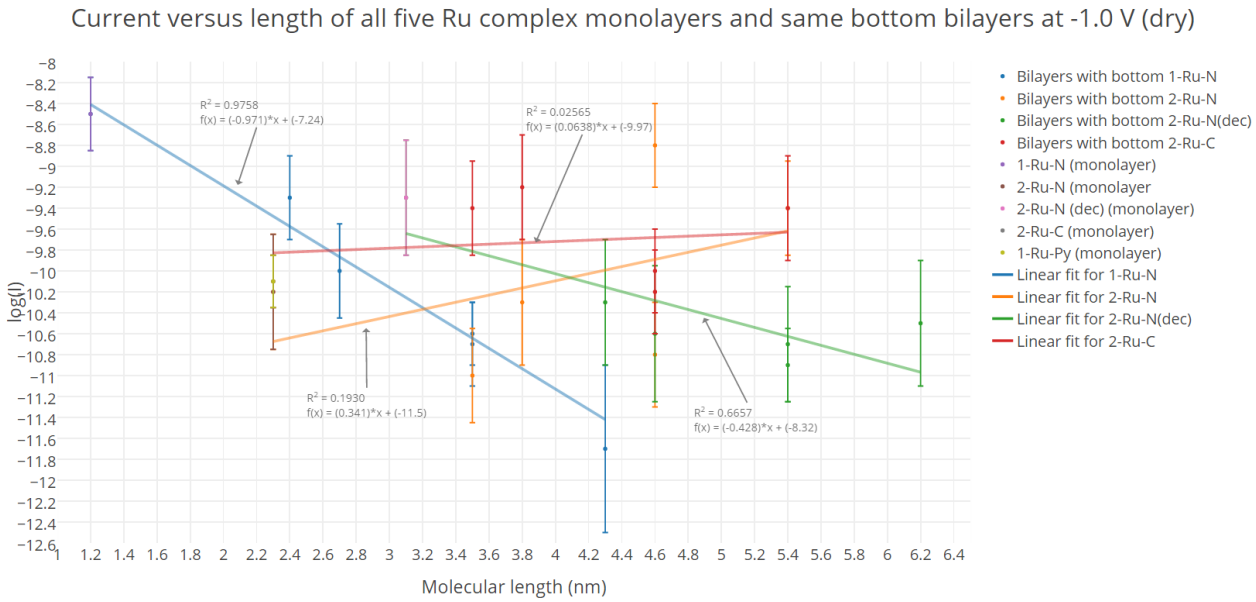

Figure 16. Semi-log plot of current versus theoretical molecular length of all Ru complex bilayers at -1.0 V and at a low RH. Linear fit values are -0.971 ± 0.076 for 1-Ru-N, 0.34 ± 0.35 for 2-Ru-N, -0.43 ± 0.15 for 2-Ru-N (dec) and 0.06 ± 0.20 for 2-Ru-C. At 4.6 nm, the current through the combination 2-Ru-N with top 2-Ru-C (-8.8 ± 0.4) is higher than that through the 2-Ru-N double layer (-10.8 ± 0.5).

The bilayers with bottom layer 2-Ru-N(dec) (and with bottom 1-Ru-N, as discussed) have current values that suit with the theory of the length dependent conductance, i.e. their conductance decreases exponentially with their length without the combination of molecules being an important parameter.

log(I) @-1.0 V (dry)						
	Bottom					
Top		1-Ru-N	2-Ru-N	2-Ru-N(dec)	2-Ru-C	1-Ru-Py
	1-Ru-N	-9.3±0.4	-10.7±0.4	-11.7±0.8	-10.6±0.3	-10.0±0.45
	2-Ru-N	-11.0±0.45	-10.8±0.5	-9.4±0.45	-8.8±0.4	-10.3±0.6
	2-Ru-N(dec)	-10.3±0.6	-10.9±0.35	-10.5±0.6	-10.7±0.55	-10.6±0.65
	2-Ru-C	-9.4±0.45	-10.2±0.4	-9.4±0.5	-10.0±0.4	-9.2±0.5

Table 1. The current values of the bilayers consisting of the same molecules are given the same color. Each combination has different current values than its inverse, except for the combinations of 1-Ru-N with 2-Ru-N (colored red). The entries for the double layers consisting of the same molecules are colored grey and those for the bilayers with top molecule 1-Ru-Py (which have no inverse combination) are colored blue.

At a high RH, the slope of the linear fit for the bilayers with 2-Ru-N is still positive, even a bit steeper than in the dry case but with overlapping error bars (see fig. 17). The combinations with top molecules 2-Ru-N and 1-Ru-Py have a significant lower current than at a low RH, but we are not sure if these measurements are reliable because of their extraordinary low current values in the humid case compared to other measurements. The 2-Ru-N double layer has a much lower current value at this voltage than at low RH (see table 2 as well as table 1), due to rectification. The combinations with bottom molecule 2-Ru-C still have a high conductance for their length, except for the double layer and the one with top molecule 2-Ru-N – just like in the dry case. Furthermore, we see that the values for the combinations with bottom molecule 2-Ru-N(dec) again have a negative slope (even with a higher sloop but still within the same error range as at a low RH). The combination with top molecule 1-Ru-Py however, seems to have a higher conductance.

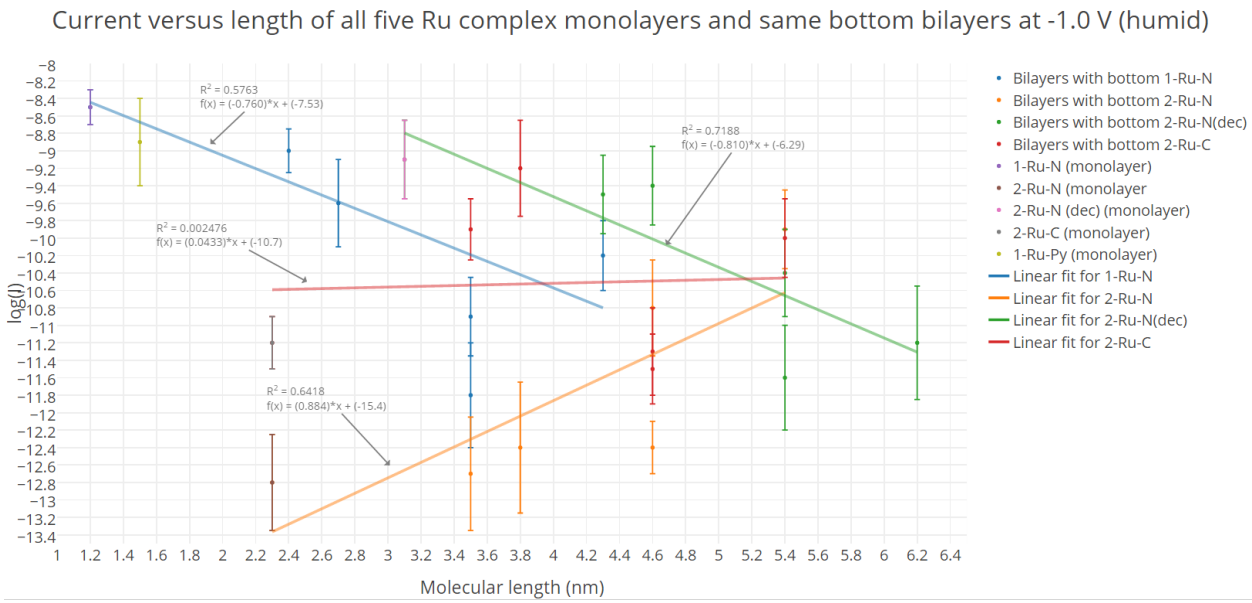

Figure 17. Semi-log plot of current versus theoretical molecular length of all Ru complex bilayers at -1.0 V and at a high RH. Linear fit values are -0.76 ± 0.23 for 1-Ru-N, 0.88 ± 0.33 for 2-Ru-N, -0.81 ± 0.25 for 2-Ru-N (dec) and 0.04 ± 0.43 for 2-Ru-C. The 2-Ru-N double layer has a current value of -12.4 ± 0.3.

In the table below we compare the current values of the combinations with those of their inverse ones again, but now at a high RH.

log(I) @-1.0 V @humid						
	Bottom					
Top		1-Ru-N	2-Ru-N	2-Ru-N(dec)	2-Ru-C	1-Ru-Py
	1-Ru-N	-9.0±0.25	-11.8±0.6	-10.2±0.4	-10.9±0.45	-9.7±0.5
	2-Ru-N	-12.7±0.65	-12.4±0.3	-9.9±0.45	-10.8±0.55	-12.3±0.75
	2-Ru-N(dec)	-9.5±0.45	-11.6±0.6	-11.2±0.65	-10.4±0.5	-9.4±0.45
	2-Ru-C	-9.9±0.35	-11.5±0.4	-10.0±0.45	-11.3±0.5	-9.8±0.55

Table 2. Almost every combination could have the same current value as their inverse (given their error bars), these are colored red. The exceptions for this that do have a different conductance when inversed are the combinations of 1-Ru-N with 2-Ru-C and 2-Ru-N with 2-Ru-N(dec). The entries for the double layers consisting of the same molecules are colored grey and those for the bilayers with top molecule 1-Ru-Py are colored blue. The other current values of the bilayers consisting of the same molecules are given the same color.

Taking the observations above into account, we can conclude that the bilayers with bottom molecules 1-Ru-N and 2-Ru-N(dec) have a conductance that exponentially decreases with the length of the combination. Surprisingly enough, those with bottom layers 2-Ru-N and (to a lesser extent) 2-Ru-C have a weak length dependence, as there are combinations with higher current values while the length of these bilayers is also greater than those with lower current values. While we have seen in section 1.3 that there exist Ru complex wires with a weak length dependence[13], it was not expected that some bottom layers show a clear length dependent conductance while other molecules with a different bottom molecular layer do not. We have no explanation for this yet and further research is recommended.
At a low RH, the current values at -1.0 V all differ from those of inverse combinations (see table 1), except for the combinations consisting of a 1-Ru-N SAM and a 2-Ru-N SAM.

In the humid case, rectification is an important factor for the conductance (especially in these figures because the RR is maximum around 1.0 V for most of the measured bilayers). Also, the combinations with almost no rectification at that voltage do not have a significantly different current at a high RH compared to the dry case (see for example the current values in table 1 and table 2 of the combinations with bottom/top molecular layer 2-Ru-N/2-Ru-N(dec) and the combination 1-Ru-N/2-Ru-C with a low RR at -1.0 V according to table 3). Therefore, it is safe to say that the conductance only depends on the humidity in the sense that rectification determines if the current values are higher than at a low RH.

3.4.1 Comparison of bilayers to monolayers with the same bottom

In Appendix C, the I-V characteristics of self-assembled monolayers that consist of the used molecules in this experiment are shown, again at a low and high RH. As in Appendix D, the RR is calculated and plotted against the bias voltage. We use this to make a short, qualitative comparison between the shape of the I-V curves of self-assembled bilayers and that of the self-assembled monolayers that have the same bottom molecular layer. Only the I-V curves and RR plots at a high RH are compared, as practically all combinations have symmetric I-V curves at a low RH.

Starting with 1-Ru-N, we see that the I-V curve of the double layer and the bilayer with top 1-Ru-Py have are comparable to that of the monolayer. However, the RR of the double layer at 1.0 V is higher. The direction of rectification is still the same. In the case of 2-Ru-N, none of the bilayers have a shape that is similar to that of the monolayer due to the very high RR of the 2-Ru-N SAM. The double layer is also quite different, showing hysteretic effects. The ones with top layer 1-Ru-N or 2-Ru-C come the closest to this regarding the shape of their I-V curves. Furthermore, the double layer consisting of 2-Ru-N(dec) molecules and (to a lesser extent) the bilayers with the same bottom molecules but top layers 2-Ru-C or 1-Ru-Py look similar. Lastly, none of the bilayers with bottom molecules 2-Ru-C have an I-V curve that is comparable to that of the 2-Ru-C SAM, due to its ‘nod’ around -0.3 V.

3.5 Length and humidity dependence of conductance of SAMTs with top 1-Ru-N

These sections contains the same data sets as the previous two, but here we present them in a different way. By grouping the bilayers with the same top molecule and comparing the findings with those in the previous section, we might be able to spot a pattern. It should be noted that there is one data point less per group and there are five groups instead of four, because of the fact that is not possible to create bilayers with 1-Ru-Py as bottom molecule. The linear fits for the multilayers consisting of 1-Ru-N molecules are included again in the first two plots, but we will not discuss those as this has already been done previously (in section 3.3).

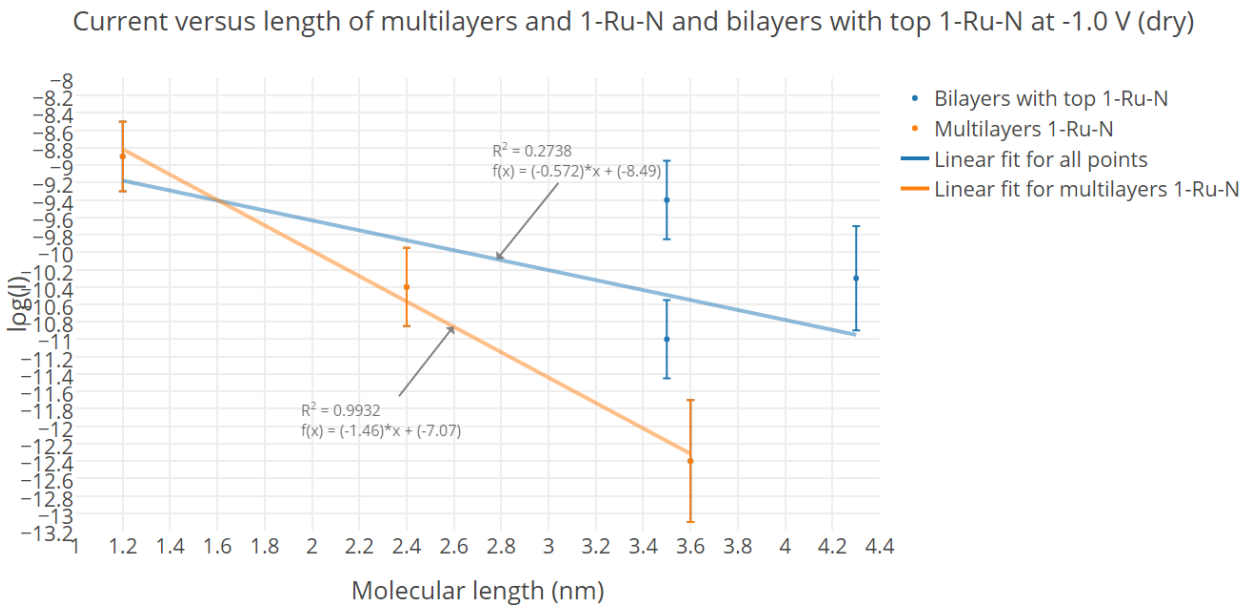

Figure 18. Semi-log plot of the current versus theoretical molecular length of multilayers 1-Ru-N (up to three layers) and bilayers with top 1-Ru-N at -1.0 V and at a low RH. The multilayers are colored orange, while the combinations with bottom layer 1-Ru-N are colored blue. The linear fit for the multilayers has a slope of -1.46 ± 0.31 nm-1 (as already shown in figure 12) and the fit for all data points (multilayers as well as bilayers with top 1-Ru-N) has a slope of -0.57 ± 0.38 nm-1.

In the plot in fig.18 we see that the data points of bilayers with a different bottom molecule than 1-Ru-N all deviate from the linear fit, which was not the case for those of the bilayers each with bottom molecule 1-Ru-N. As there is no rectification at a low RH, this could mean that bilayers with top molecules 1-Ru-N have a conductance that depends more on the molecules than the length of the combination.

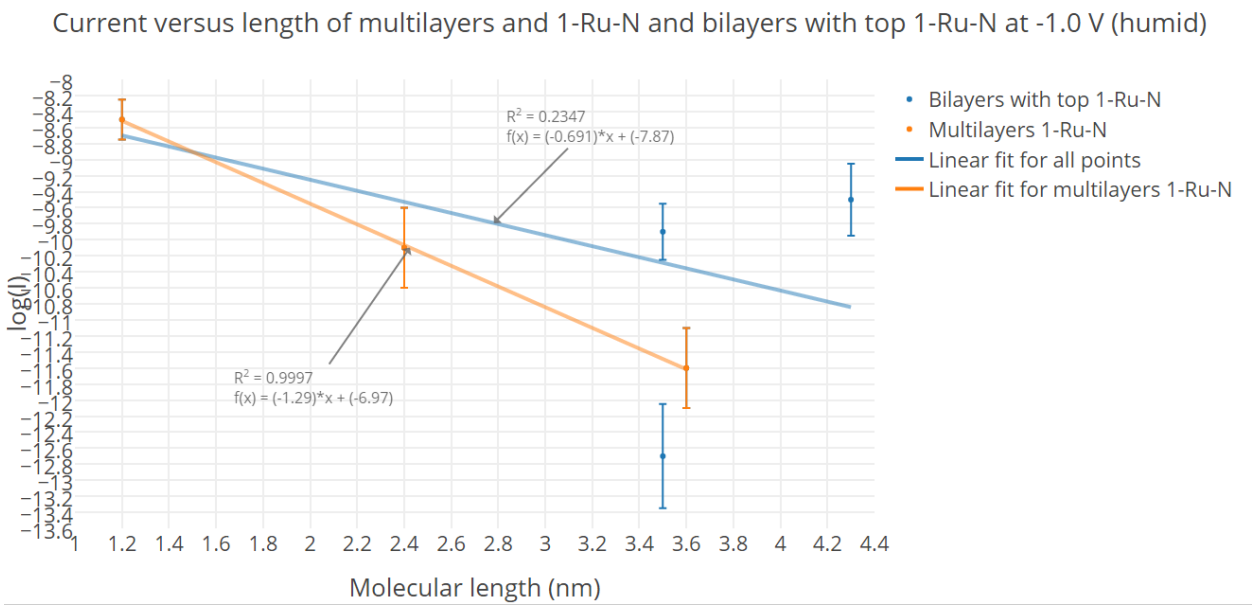

Figure 19. Semi-log plot of the current versus theoretical molecular length of multilayers 1-Ru-N (up to three layers) and bilayers with top 1-Ru-N at -1.0 V and at a low RH. The multilayers are colored orange, while the combinations with bottom layer 1-Ru-N are colored blue. The linear fit for the multilayers has a slope of -1.292 ± 0.024 nm-1 (as already shown in figure 15) and the fit for all data points (multilayers as well as bilayers with top 1-Ru-N) has a slope of -0.69 ± 0.37 nm-1.

At a high RH, the current values do not seem to change regarding the error bars, except for the combination with bottom 2-Ru-N which we have treated before.

3.6 Length and humidity dependence of conductance of bilayers with the same top

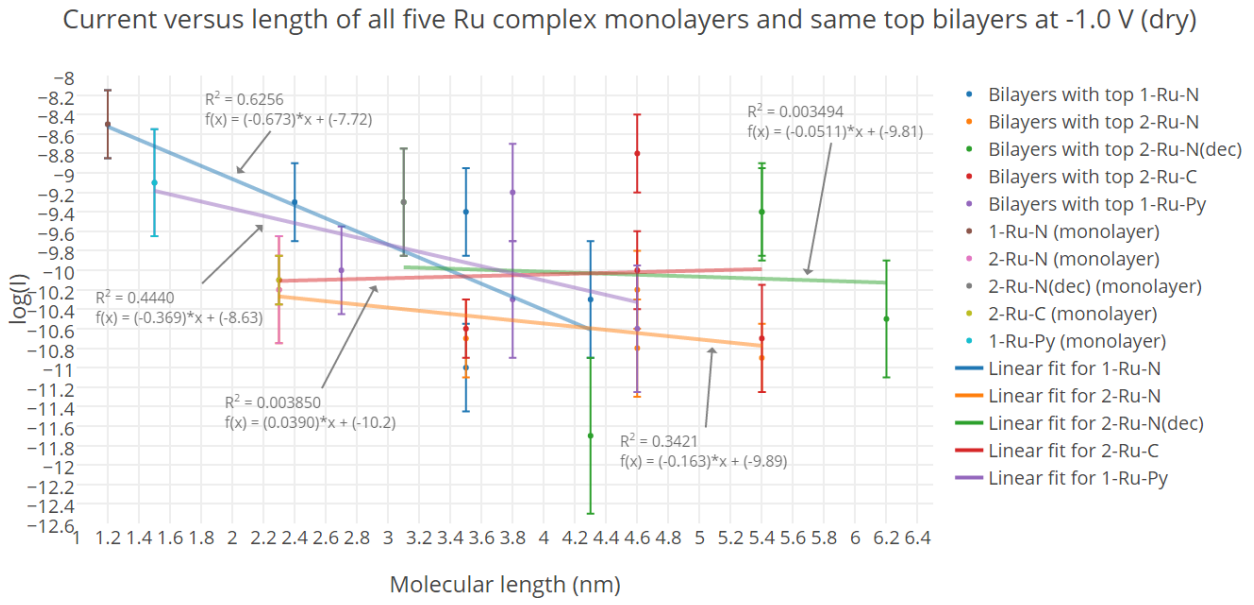

Figure 20. Semi-log plot of current versus theoretical molecular length of all Ru complex mono- and bilayers at -1.0 V and at a low RH. Linear fit values are -0.67 ± 0.26 for 1-Ru-N, -0.16 ± 0.13 for 2-Ru-N, -0.05 ± 0.50 for 2-Ru-N (dec), 0.04 ± 0.36 for 2-Ru-C, -0.37 ± 0.24 for 1-Ru-Py.

We again look for deviating data points on the plot with combinations with the same top molecules (see fig. 20). We see that all current values for the bilayers with top 2-Ru-N(dec) deviate and all but one for those with 2-Ru-C. The error bars of the bilayers with bottom layer 2-Ru-C and 2-Ru-N and top layer 1-Ru-N (both at 3.5 nm) also do not overlap the linear fit for 1-Ru-N. The bilayers with the other two

molecules on top have only one deviating data point each. The length dependence of the conductance that we have seen in section 3.4 for bilayers with the same bottom molecular layer in the dry case (see fig. 16) does not appear for bilayers with the same top molecular layer.

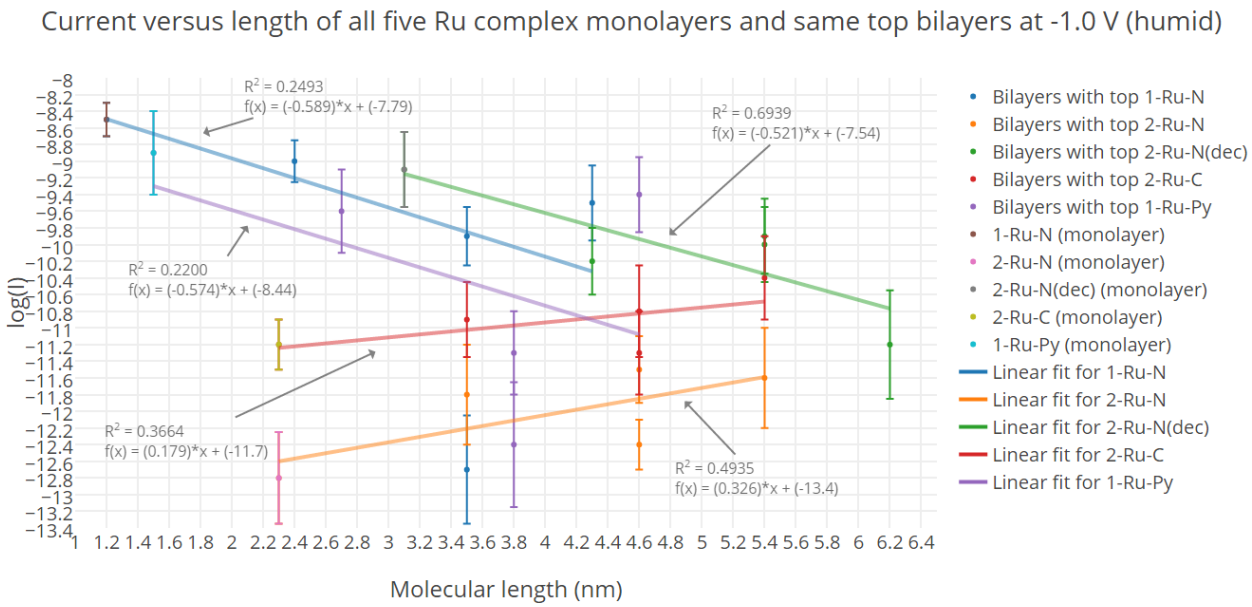

Figure 21. Semi-log plot of current versus theoretical molecular length of all Ru complex mono- and bilayers at -1.0 V and at a high RH. Linear fit values are -0.59 ± 0.34 for 1-Ru-N, 0.33 ± 0.19 for 2-Ru-N, -0.52 ± 0.20 for 2-Ru-N (dec), 0.18 ± 0.14 for 2-Ru-C, -0.57 ± 0.62 for 1-Ru-Py.

In fig. 21 we again see that the combinations with a distinct rectification have different current values at a high RH, so the linear fits are more separated from each other in this plot compared to fig. 20. At the same time, the conductance of combinations without a high RR (log(RR) ≤ 0.5) does not change as we suspected before. In this case we see that almost all data points are on the linear fit for the current values at a high RH. This is similar to fig. 17, where the combinations with the same bottom molecular layers are grouped.

3.7 Rectification ratio with grouped bottom molecules at 1.0 V

In the previous four sections, we have analyzed the measurements on the 20 bilayers by comparing their current values at -1.0 V with each other at a low and at a high RH. This, of course, does not tell the whole story as almost all I-V curves become asymmetric at a high RH. We take the values for this rectification as the ratio between the current at -1.0 V and at 1.0 V and plot these in groups with combinations that have the same bottom or top molecule. In that way, we get an overview of the magnitude of the calculated rectification ratio for each bilayer at 1.0 V. Furthermore, we can look again for a pattern. The reason that we look at the RR at 1.0 V, aside from the fact that we compared the current values at -1.0 V, is that for most of the bilayers (9 out of 20) the bias voltage at which the RR is maximum is around 0.9 V.

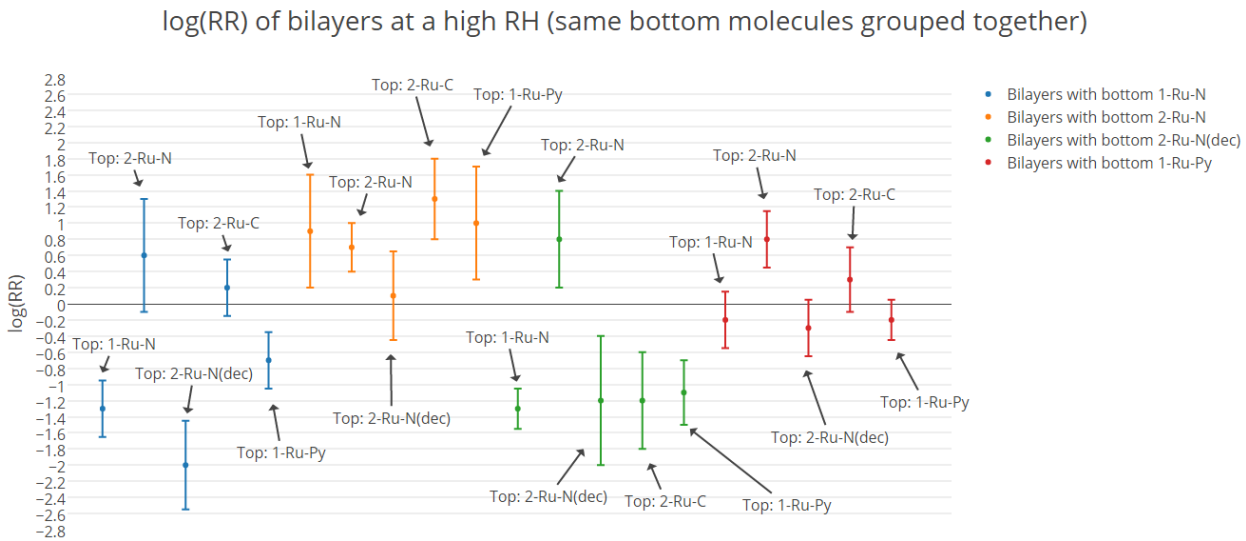

Figure 22. Semi-log plot of the rectification ratio at 1.0 V for each bilayer. Bilayers with the same bottom molecule are grouped together.

We see that bilayers with bottom molecule 2-Ru-N all have a fairly positive log(RR), the only exception being the one with top layer 2-Ru-N(dec), which could be negative. The ratios of other bilayers vary more, the greatest difference being between those with bottom 1-Ru-N and top 2-Ru-N/2-Ru-N(dec). A notable feature of this graph is that the combinations with a molecular layer that consists of 2-Ru-N molecules have a positive log(RR) (higher current at a positive bias voltage than at a negative bias voltage), while the combinations with a molecular layer consisting of 2-Ru-N(dec) molecules tend to have a more negative log(RR).

log(RR) at ± 1.0 V (humid)						
	Bottom					
Top		1-Ru-N	2-Ru-N	2-Ru-N(dec)	2-Ru-C	1-Ru-Py
	1-Ru-N	-1.3±0.35	0.6±0.7	-2.0±0.55	0.2±0.35	-0.7±0.35
	2-Ru-N	0.9±0.7	0.7±0.3	0.1±0.55	1.3±0.5	1.0±0.7
	2-Ru-N(dec)	-1.3±0.25	0.8±0.6	-1.2±0.8	-1.2±0.6	-1.1±0.4
	2-Ru-C	-0.2±0.35	0.8±0.35	-0.3±0.35	0.3±0.4	-0.2±0.25

Table 3. The rectification ratio at 1.0 V for each combination is shown. The entries for the double layers consisting of the same molecules are colored light grey and those for the bilayers with top molecule 1-Ru-Py are colored light blue. By comparison, almost all of the combinations seem to have a RR that is close to that of its inverse.

In table 3 we see the rectification ratios again, but the entries with bilayers that consists of the same molecules now have the same color for comparison. Surprisingly enough, all combinations have a RR with the same sign as their inverse, which means that they both have a higher conductance in the same current direction. In addition, the RR of a combination always has a comparable value when the error bars are taken into account.

3.8 Rectification ratio with grouped top molecules at 1.0 V

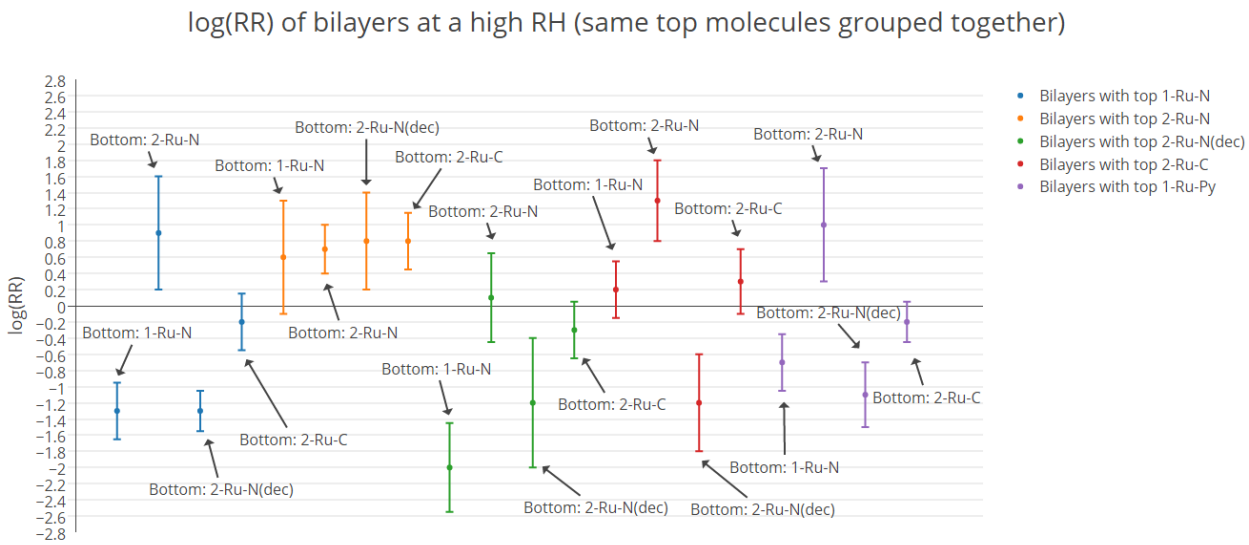

Figure 23. Semi-log plot of the rectification ratio at 1.0 V for each bilayer. Bilayers with the same top molecule are grouped together.

In this plot (see fig. 23) the combinations with the same top molecular layer are grouped together. Now we see that all combinations with top layer 2-Ru-N have a positive log(RR). Bilayers with top molecules 2-Ru-C have a slightly positive rectification ratio too, except for the combination with bottom molecules 2-Ru-N(dec). Compared to fig. 22 and regarding table 3, we see again that combinations with a molecular layer consisting of 2-Ru-N or 2-Ru-N(dec) molecules tend to have a positive and negative value of log(RR) respectively.

3.9 Final discussion

Looking back at the predictions that we have made in section 1.5, we see that almost all results turned out to be different than expected. While the I-V curves of double layers consisting of 1-Ru-N or 2-Ru-N(dec) looked similar to those of their monolayers, the ones of double layers consisting of 2-Ru-N or 2-Ru-C molecules did not. The other bilayers had I-V curves that were not always similar to (the average of) those of the SAMs of which they consist. Sometimes the RR was higher than each SAM apart, sometimes not. Three samples showed hysteretic behavior, which we did not expect. The current values at -1.0 V of the bilayers turned out to be higher than those of the SAMs for some combinations, especially for the bilayers with a bottom molecular layer consisting of 2-Ru-N or 2-Ru-C molecules, which we also did not expect. However, further research is needed to confirm if this means that the length dependence of conductance is weak for those combinations. Furthermore, except for one combination all combinations showed comparable current values at -1.0 V compared to their inverse combinations. The most unexpected result was the fact that the RR of the bilayers had the same sign and was for most combinations comparable to that of their inverse combination. All together, there were less symmetry between the I-V curves of the combinations and those of their inverse combinations than expected.

Conclusion

In summary, we have measured the I-V characteristics of 20 bilayers consisting of Ru-complex molecules at high and low RH using C-AFM. Just like in the experiment conducted by H. Atesci, V. Kaliginedi et al.[8], the I-V characteristics changed when the RH was increased from a low (≈5%) to a high (≈50%) RH.

Three samples with bilayers, namely that with double layer 2-Ru-N, bottom layer 2-Ru-N(dec) and top layer 1-Ru-N and the one with bottom layer 2-Ru-N(dec) and top layer 2-Ru-N, showed hysteretic behavior each at a specific voltage range. 8 samples (possibly more regarding their error bars) have a RR>10 at 1.0 V and at a high RH with different directions of rectification.

The highest RR found is $RR_{humid} = 10^{-2.0\pm0.55}$ at 1.0 V for the combination with bottom layer 1-Ru-N and top layer 2-Ru-N(dec). The sample with an opposite direction of rectification (with higher current values at a positive applied bias voltage) consists of a bottom layer 2-Ru-N and top layer 2-Ru-C with $RR_{humid} = 10^{1.35\pm0.6}$ at 0.9 V.

Bilayers with bottom molecules 1-Ru-N and 2-Ru-N(dec) have a conductance that exponentially decreases with the length of the combination. On the other hand, bilayers with bottom molecules 2-Ru-N and (to a lesser extent) 2-Ru-C have a weak length dependence, as the combinations of molecules seem to be an more important factor for their conductance than their total length. There is no length dependence found for bilayers with the same top molecules. Further research is required to verify the length dependence of conductance of bilayers that consist of the Ru-complex that we have used.

In the dry case, the current values at -1.0 V all differ from those of inverse combinations, except for the combinations consisting of a 1-Ru-N SAM and a 2-Ru-N SAM. Because of this exception, we are not sure if inverse combinations always have a different conductance. However, it is certain that the I-V characteristics of the bilayers differ from those of their inverse combinations.

Furthermore, the conductance of the measured samples is only humidity dependent in the sense that rectification is an important factor at a high RH for most of the bilayers, as the combinations with a low RR ($\log(RR)<0.5$) do not have a significantly different current at a high RH compared to the current values in the dry case.

All molecular combinations as measured have a RR with the same sign as their inverse combination at 1.0 V, which means that they both have a higher conductance in the same current direction. In addition, the RR of a combination always has a comparable value when the error bars are taken into account. Lastly, the combinations with a molecular layer consisting of 2-Ru-N or 2-Ru-N(dec) molecules tend to have a positive and negative value of log(RR) respectively.

We finish this overview of results and findings with that the fact that all I-V characteristics of the measured Ru-complex bilayers are changed when the RH is increased. None of the bilayers have exactly the same shape as the monolayers with the same bottom molecules, only a few looked similar (especially some double layers). We state that the rectifying and/or hysteretic effects adds functionality to the electronic circuit that consists of these molecular components, which could be useful in further research.

Outlook

By conducting these experiments, we learn more about charge transport in molecular junctions in the short run, which is a good motivation in the fundamental research of nanophysics. In the long run, this knowledge could be used to design functional devices (such as electronic chips or nanoscale sensors) where the active elements are only self-assembled mono- or multilayers, which are highly favored as they could be smaller up to an order of magnitude while adding functionality.

The first half of this bachelor research project was devoted to temperature dependent measurements of the conductance of 1-Ru-N multilayers. The original idea was to vary the temperature of the sample in order to look for an intrinsic transition from tunneling to hopping charge transport mechanism, which is the dominant conduction mechanism for longer molecular junctions [18]. In the hopping regime, the conductance decays linearly instead of exponentially and is temperature dependent. We expected to see a difference in current versus temperature measurements starting at multilayers with 4 or 5 layers in total. However, the conductance was too low to continue this experiment (see the measurements on the 1-Ru-N multilayers in Appendix D on p.41). Possible additional research can start with this and to this end, we give additional details on how these temperature dependent measurements were done.

We add a Peltier element to the experimental setup. We put this directly under the sample. By letting a current flow through the Peltier element, the side to which the electrons go heats up due to the thermoelectric effect. This enables us to vary the temperature of the sample from room temperature to over 70°C. When conducting temperature dependent measurements, the RH is decreased to ~ 5% so that it cannot be a second parameter that changes the conductance or the shape of the I-V curves. By exchanging the wires from the positive and negative contact on the source meter, it is also possible to cool down the sample a few degrees. Because it was not possible to attach our temperature sensor to the sample, we decided to gauge the voltage that was required to get to 25, 40, 55 and 70 degrees Celsius. In order to reach those temperatures with an error of 2 degrees, voltages of 0.75, 0.25, 0.81 and 1.21 V were applied with currents of 137, 45.4, 139 and 199 mA respectively.
We also conducted humid dependent measurements on the 1-Ru-N multilayers. However, during these the temperature of the setup was kept constant, as the relative humidity depends on the temperature. By doing so, we avoided doing measurements where more than one parameter is changed.

Besides the temperature dependent measurements, we think of humidity dependent measurements on Ru-complex SAMTs consisting of three layers. It is expected that the 80 different combinations that came be made with the same molecules as in this experiment again have I-V characteristics with interesting features. However, as the conductance seems to decrease exponentially for most of the SAMTs, it is recommended to keep it as high as possible by for example skipping the Ar etching step and using an AFM tip with a bigger tip radius.

Acknowledgements

I would like to express my great appreciation to my daily supervisor MSc. Hüseyin Atesçi, whose patience, knowledge, commitment and humor has helped me a lot during the whole project. Advice and feedback given by my supervisor dr. ir. Sense Jan van der Molen has been a great help in this experimental research. Last but not least I would like to thank MSc. Hasan Atesçi and fellow students Wouter and Bart for their presence and participation in a particular computer game we played sometimes, which has also made this research project an educational and enjoyable experience.

Appendix A

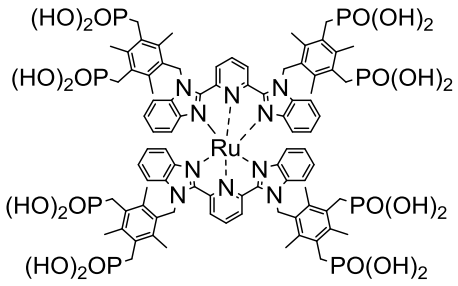

Figure 24: 1-Ru-N with charge 2+.

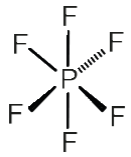

Figure 25: PF_6^- with charge -1.

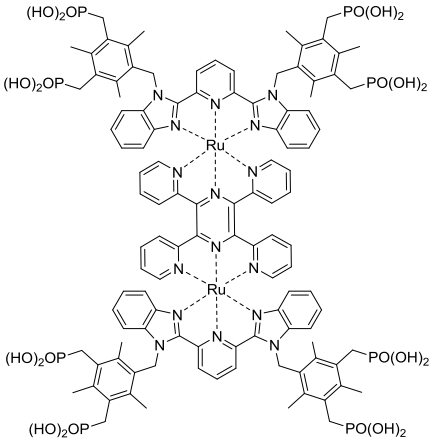

Figure 26: 2-Ru-N with charge 4+.

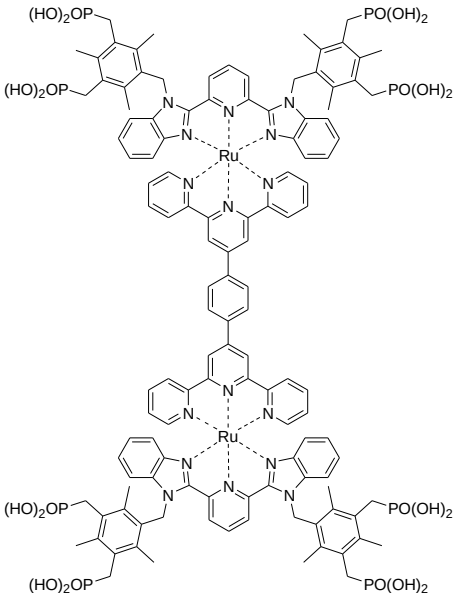

Figure 27: 2-Ru-N (decoupled) with charge 4+.

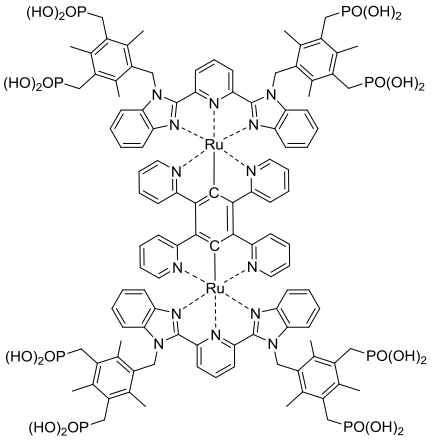

Figure 28: 2-Ru-C with charge 3+.

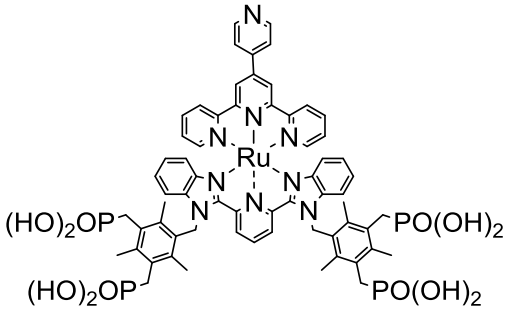

Figure 29: 1-Ru-Py with charge 2+.

Appendix B

Theoretical length of combination						
	Bottom	*1.2*	*2.3*	*3.1*	*2.3*	*1.5*
Top		1-Ru-N	2-Ru-N	2-Ru-N(dec)	2-Ru-C	1-Ru-Py
1.2	1-Ru-N	2.4	3.5	4.3	3.5	2.7
2.3	2-Ru-N	3.5	4.6	5.4	4.6	3.8
3.1	2-Ru-N(dec)	4.3	5.4	6.2	5.4	4.6
2.3	2-Ru-C	3.5	4.6	5.4	4.6	3.8
1.5	1-Ru-Py					

Table 4: The five Ru complex molecules have lengths of a few nanometers. We assume that we can add these for our measured bilayers and multilayers, and that the thickness of the $ZrCl_2O$ buffer layer between two layers can be neglected (as mentioned). The row with bottom molecule 1-Ru-Py is colored black, as a SAM consisting of these molecules is a termination layer.

Appendix C

Monolayers as measured by H. Atesci, V. Kaliginedi et al.[8]

1-Ru-N

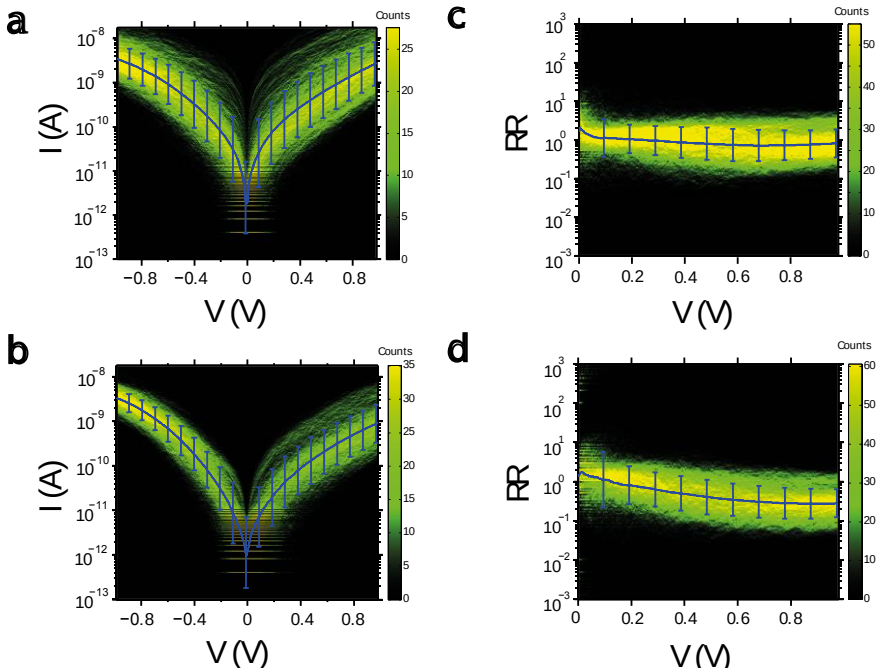

Figure 30. The figures at the top and at the bottom are obtained at a low and at a high RH respectively.

2-Ru-N

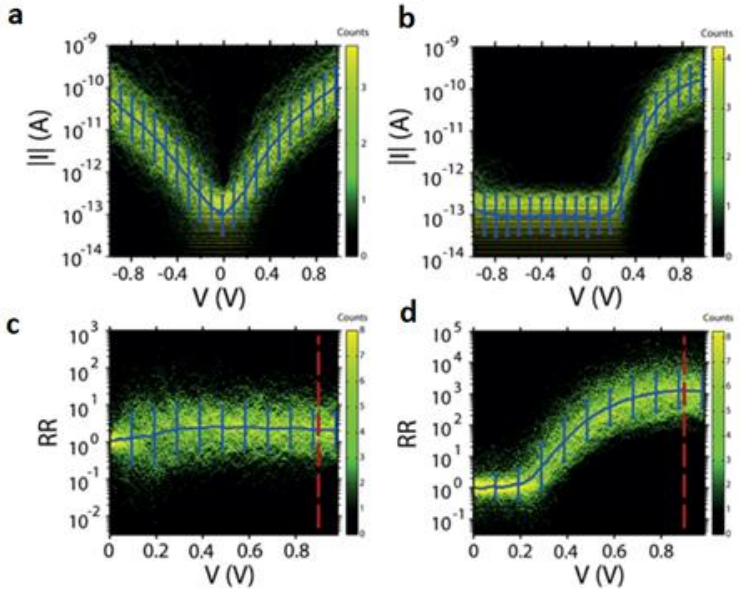

Figure 31. The figures on the left and on the right are obtained at a low and at a high RH respectively.

2-Ru-N (decoupled)

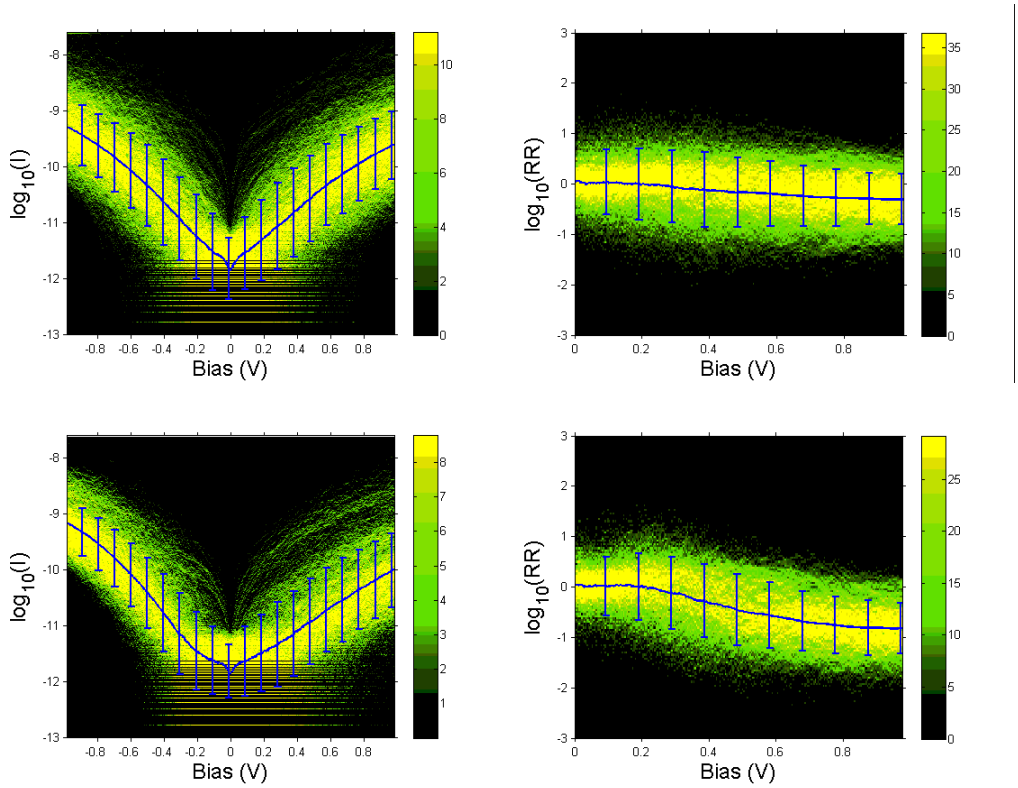

Figure 32. The figures at the top and at the bottom are obtained at a low and at a high RH respectively.

2-Ru-C

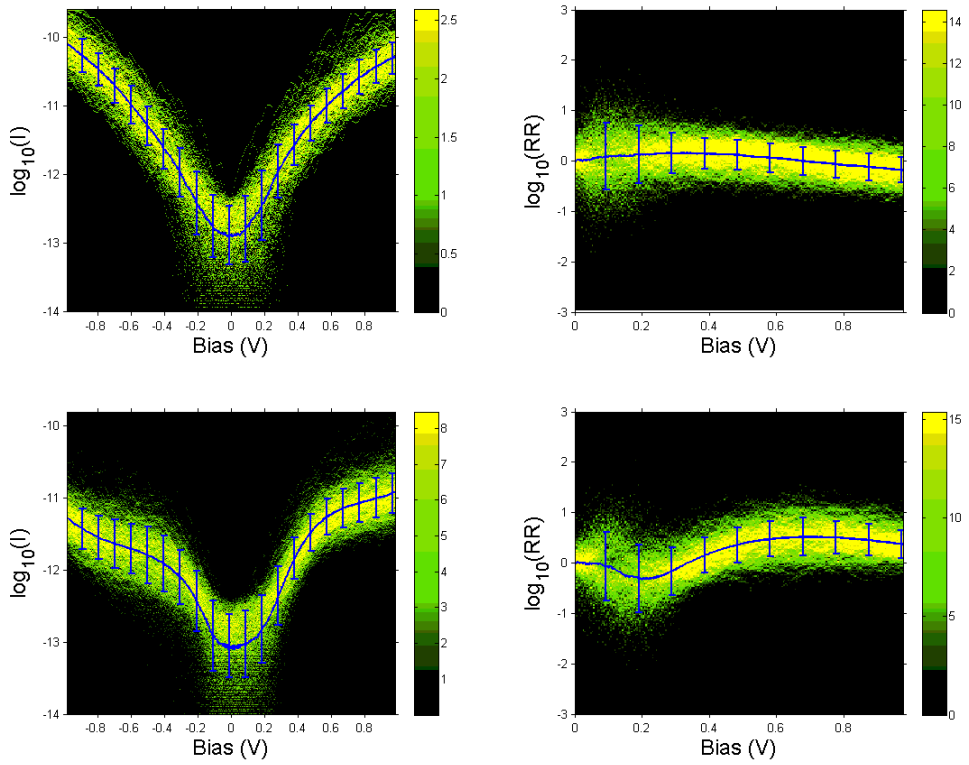

Figure 33. The figures at the top and at the bottom are obtained at a low and at a high RH respectively.

1-Ru-Py

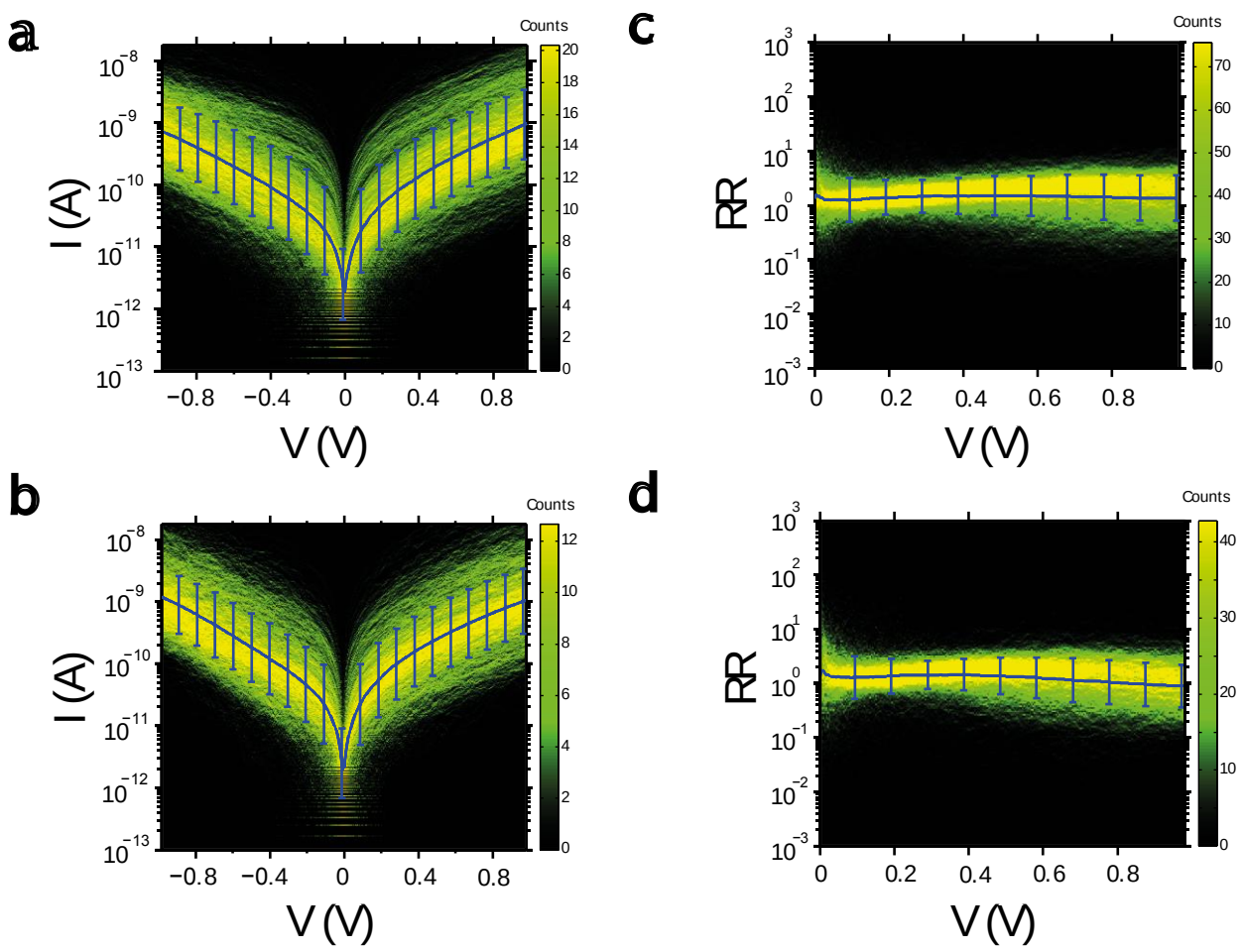

Figure 34. The figures at the top and at the bottom are obtained at a low and at a high RH respectively.

Appendix D

Bilayers with bottom molecule 1-Ru-N

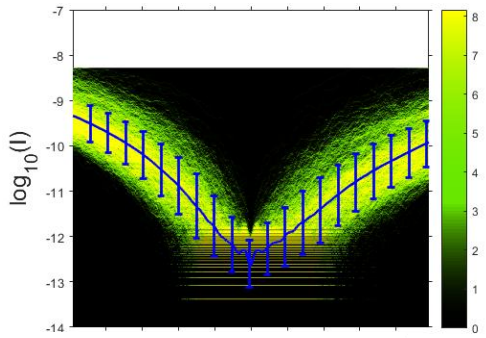

1-Ru-N double layer: low RH

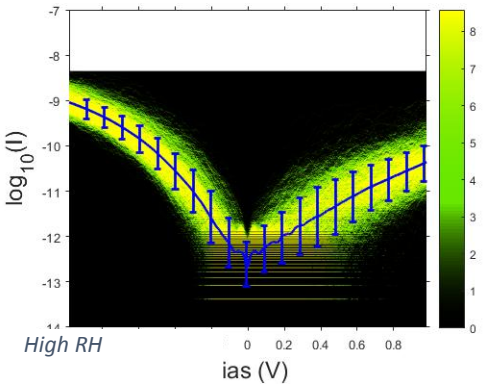

High RH

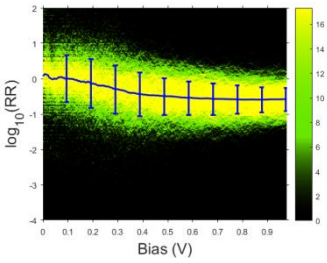

Low RH

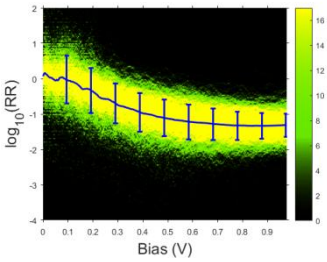

High RH

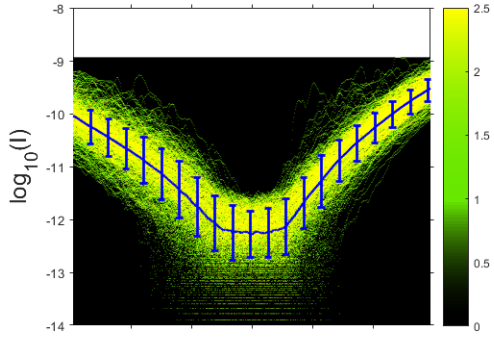

Bottom 1-Ru-N, top 2-Ru-N: low RH

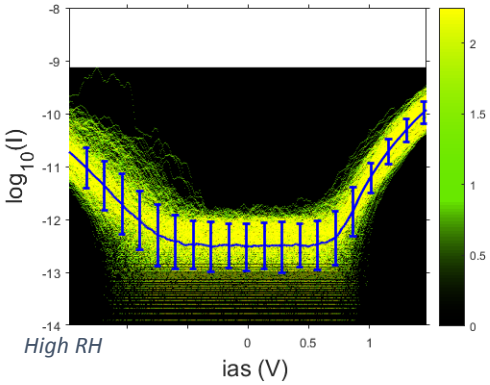

High RH

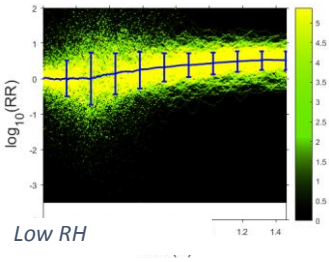

Low RH

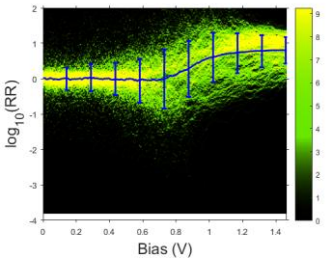

High RH

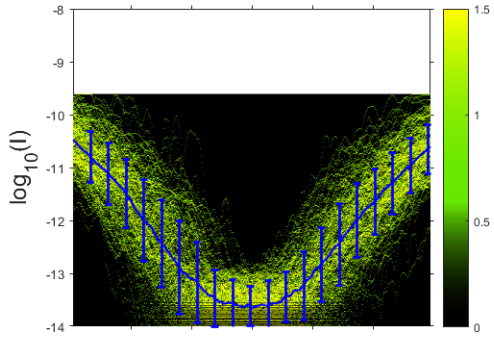

Bottom 1-Ru-N, top 2-Ru-N(dec): low RH

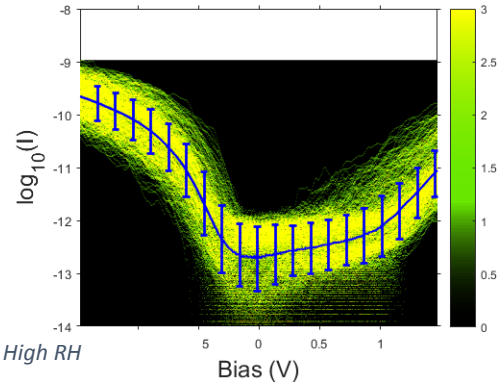

High RH

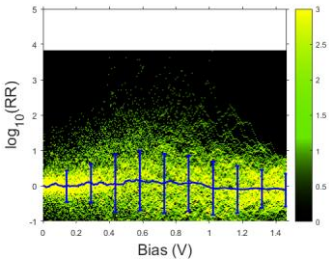

Low RH

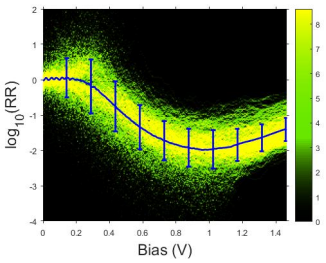

High RH

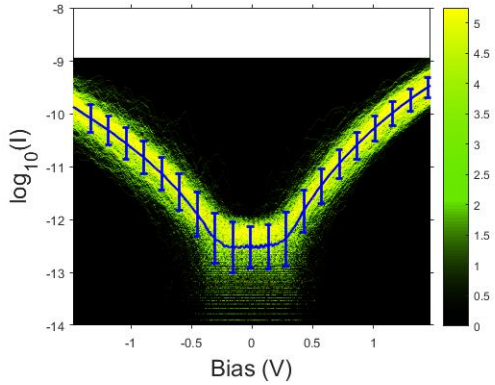

Bottom 1-Ru-N, top 2-Ru-C: low RH

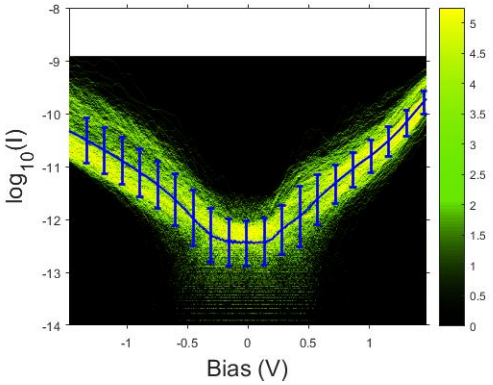

High RH

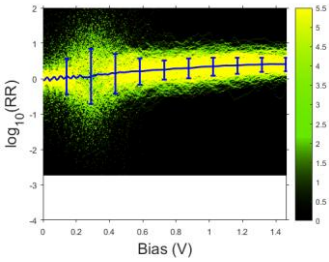

Low RH

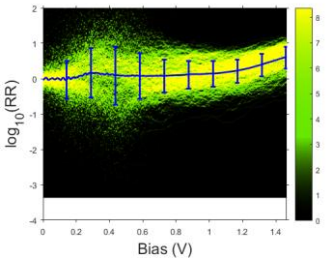

High RH

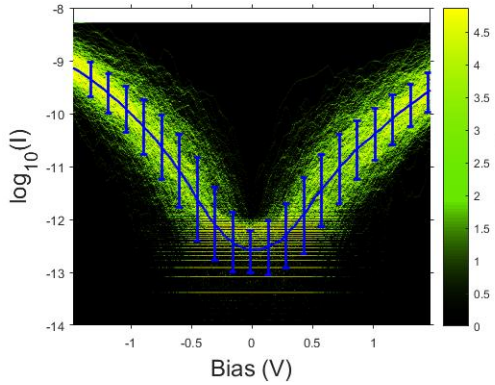

Bottom 1-Ru-N, top 1-Ru-Py: low RH

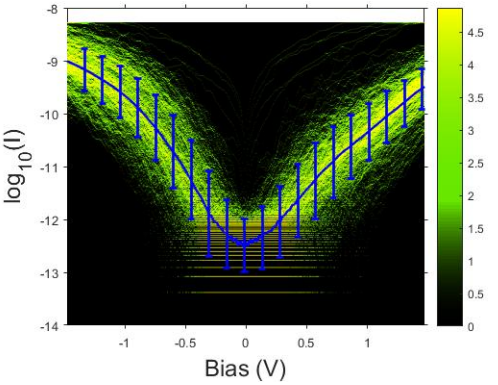

High RH

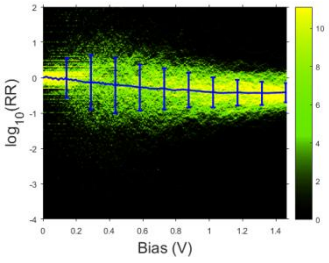

Low RH

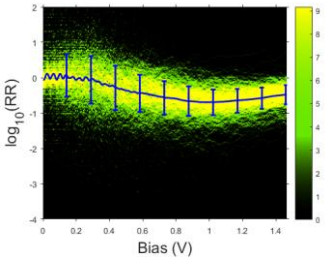

High RH

Bilayers with bottom molecule 2-Ru-N

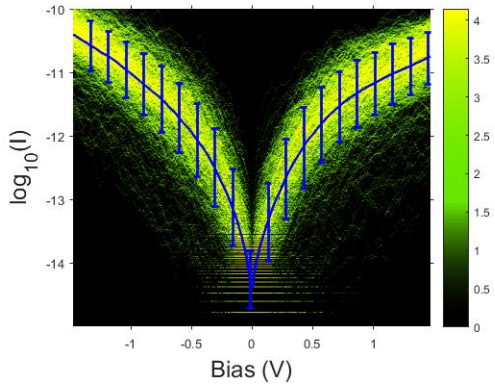

Bottom 2-Ru-N, top 1-Ru-N: low RH

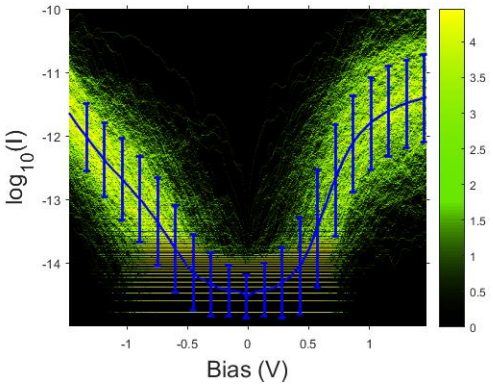

High RH

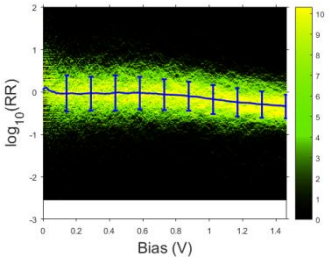

Low RH

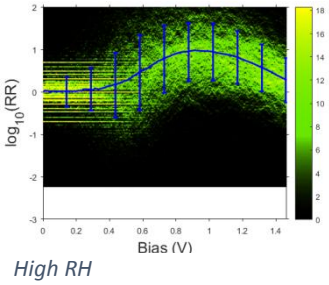

High RH

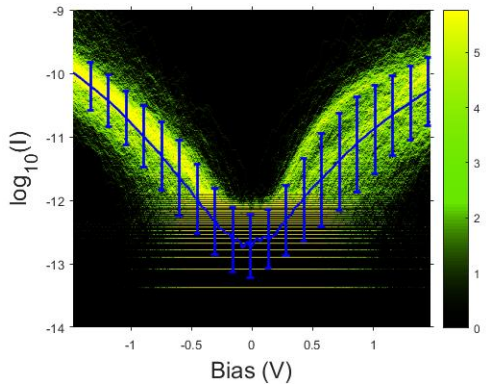

2-Ru-N double layer: low RH

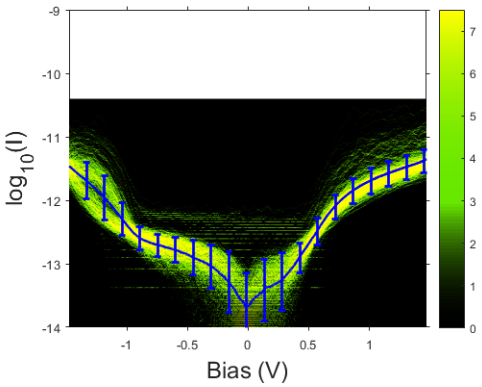

High RH

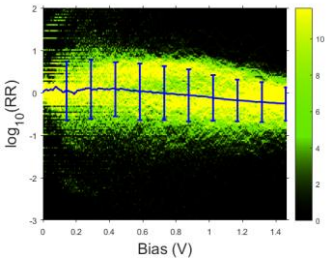

Low RH

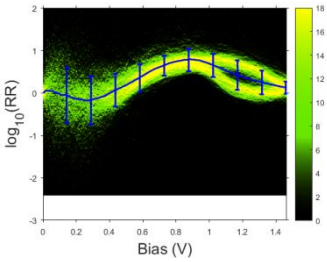

High RH

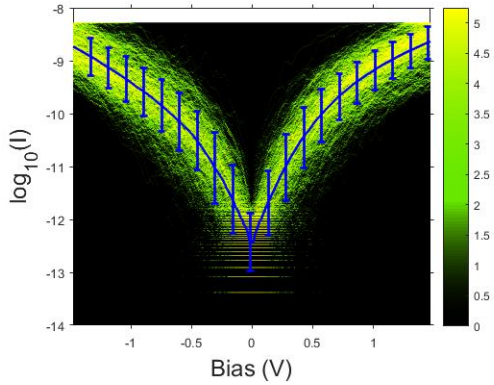

Bottom 2-Ru-N, top 2-Ru-N(dec): low RH

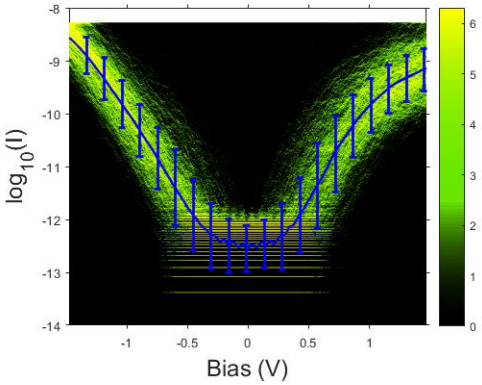

High RH

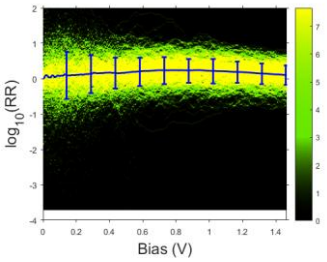

Low RH

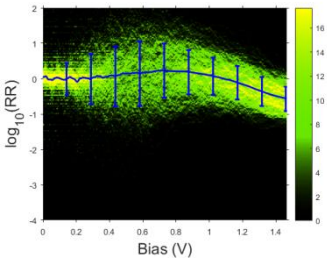

High RH

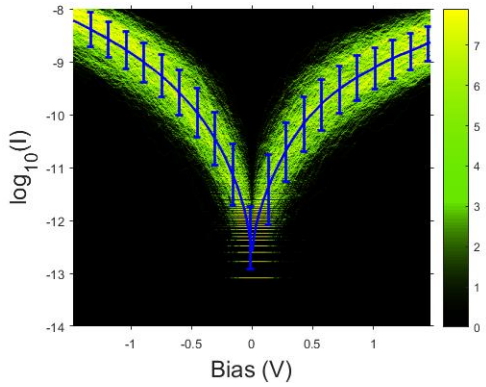

Bottom 2-Ru-N, top 2-Ru-C: low RH

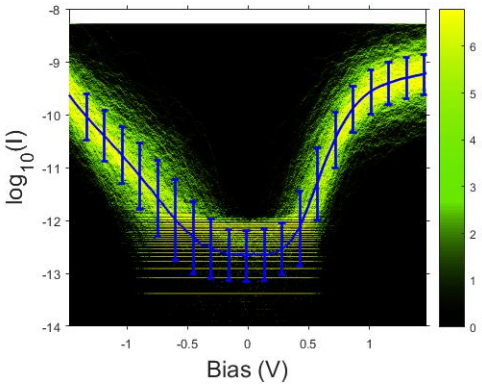

High RH

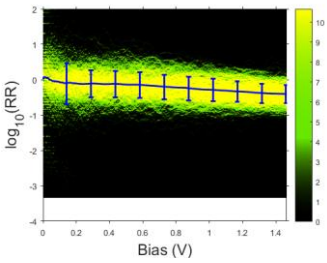

Low RH

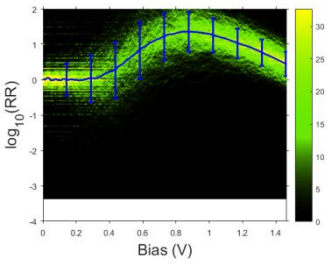

High RH

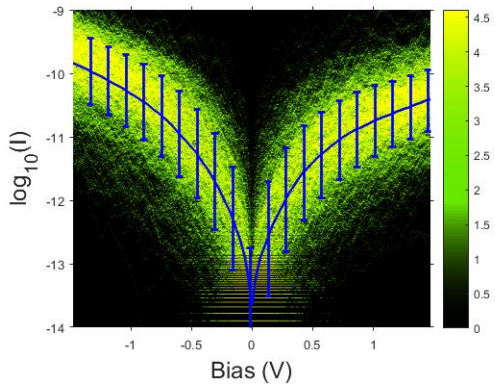

Bottom 2-Ru-N, top 1-Ru-Py: low RH

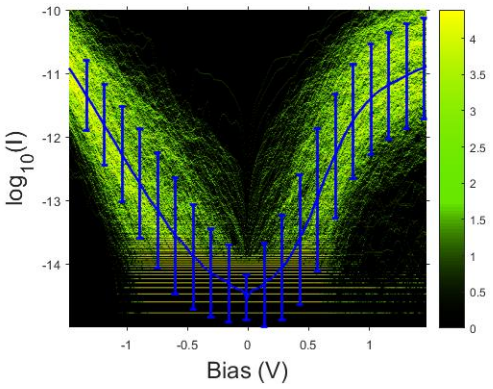

High RH

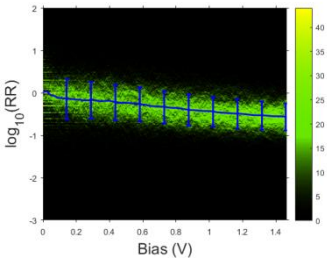

Low RH

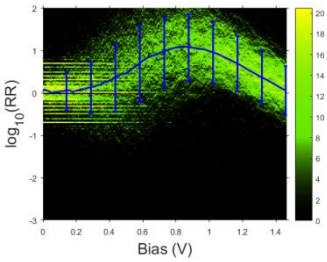

High RH

Bilayers with bottom molecule 2-Ru-N (decoupled)

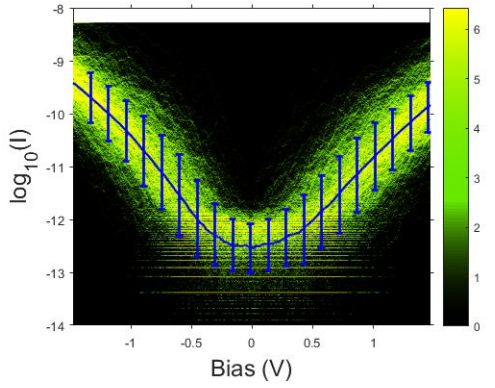

Bottom 2-Ru-N(dec), top 1-Ru-N: low RH

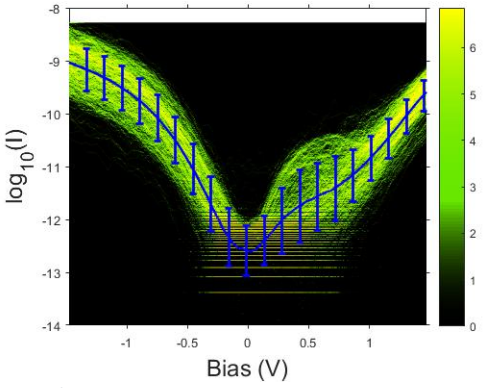

High RH

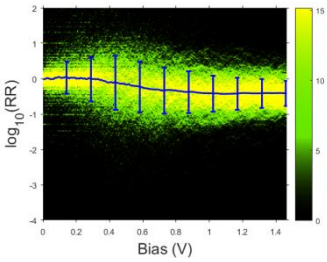

Low RH

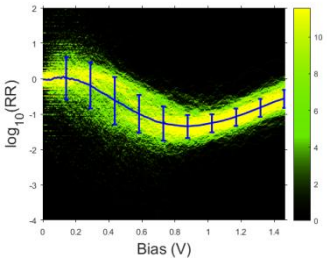

High RH

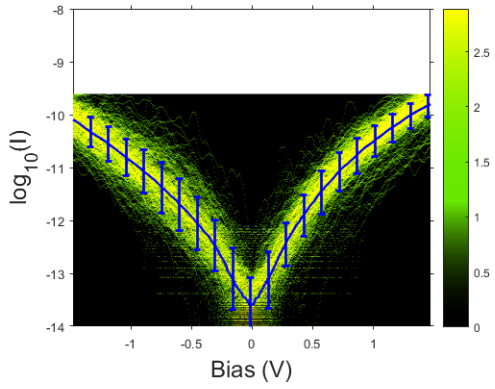

Bottom 2-Ru-N(dec), top 2-Ru-N: low RH

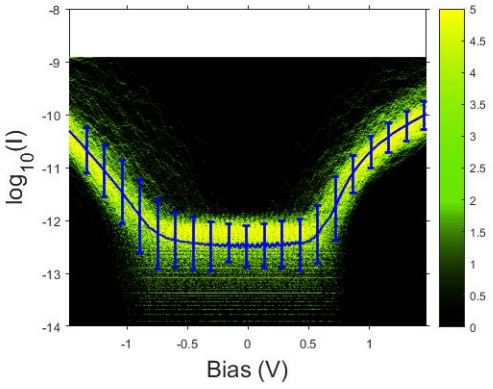

High RH

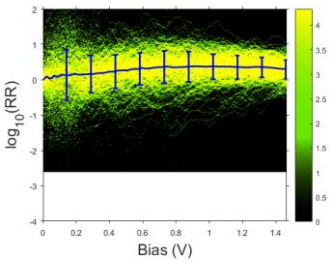

Low RH

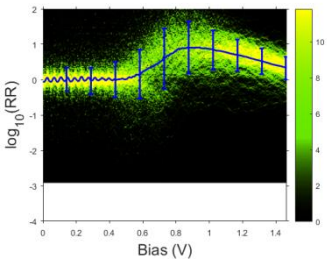

High RH

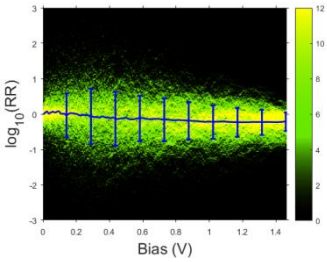

Low RH

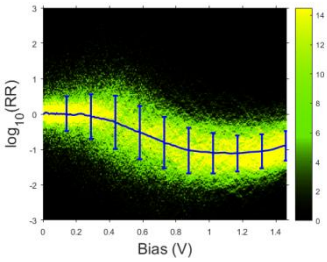

High RH

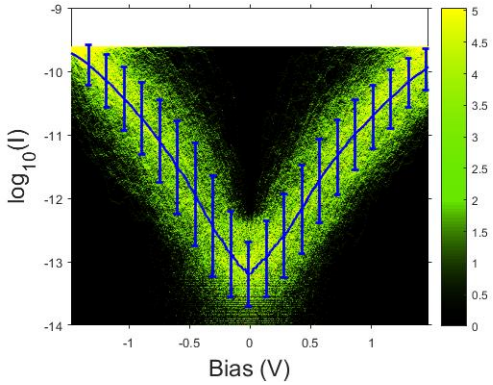

2-Ru-N(dec) double layer: low RH

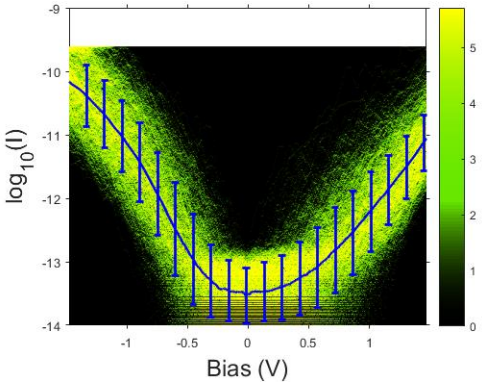

High RH

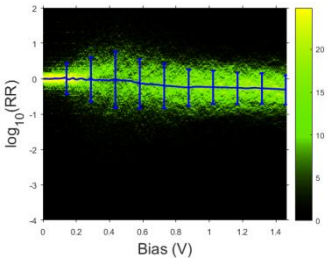

Low RH

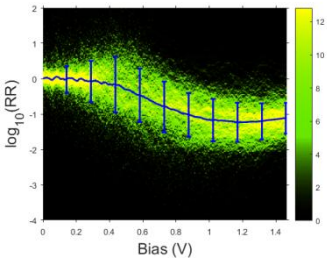

High RH

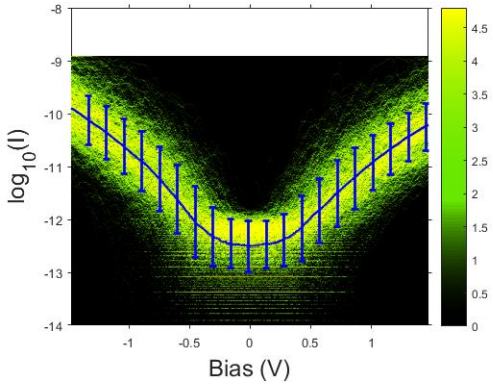

Bottom 2-Ru-N(dec), top 2-Ru-C: low RH

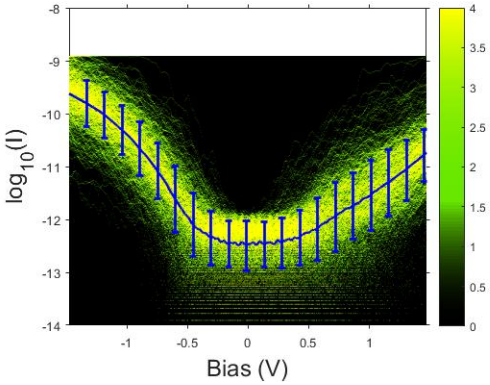

High RH

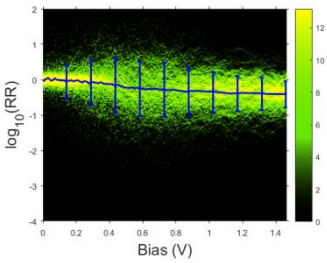

Low RH

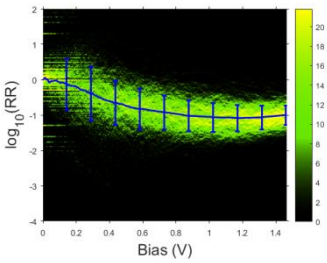

High RH

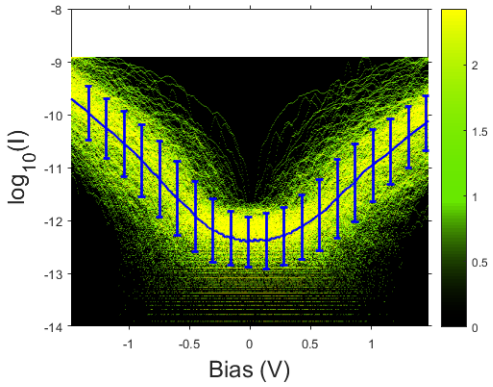

Bottom 2-Ru-N(dec), top 1-Ru-Py: low RH

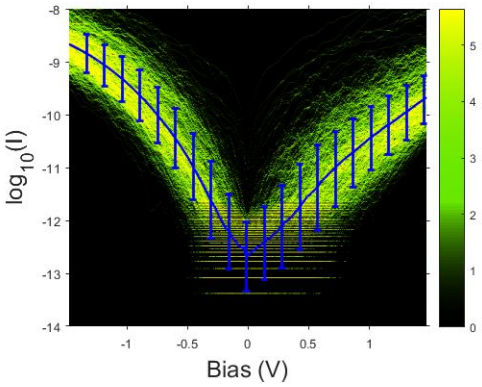

High RH

Bilayers with bottom molecule 2-Ru-C

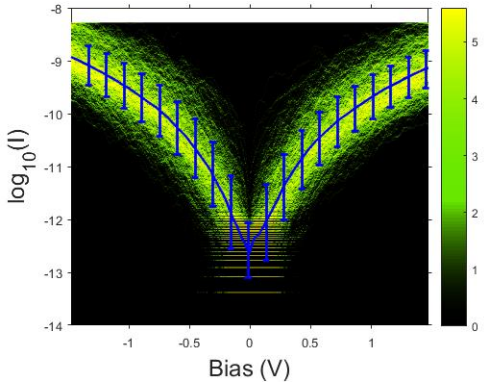

Bottom 2-Ru-C, top 1-Ru-N: low RH

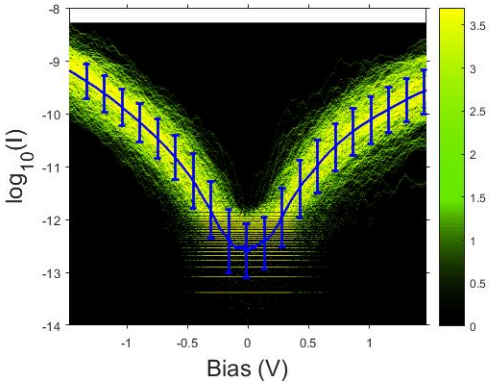

High RH

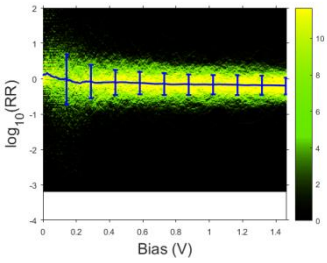

Low RH

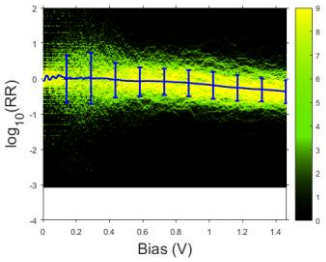

High RH

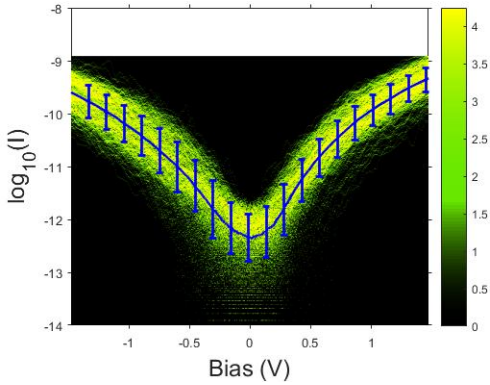

Bottom 2-Ru-C, top 2-Ru-N: low RH

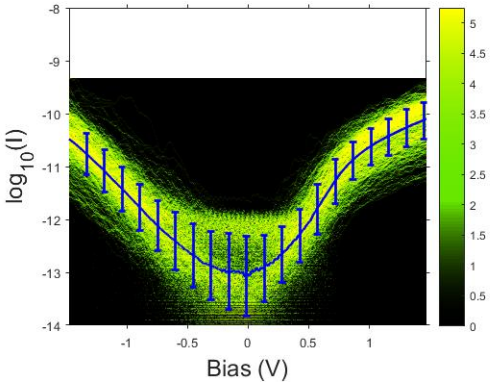

High RH

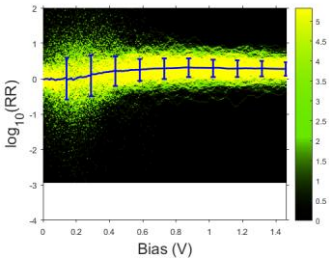

Low RH

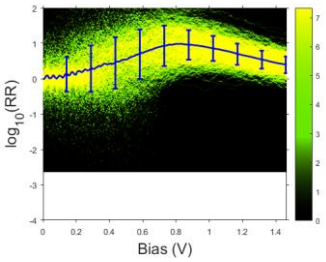

High RH

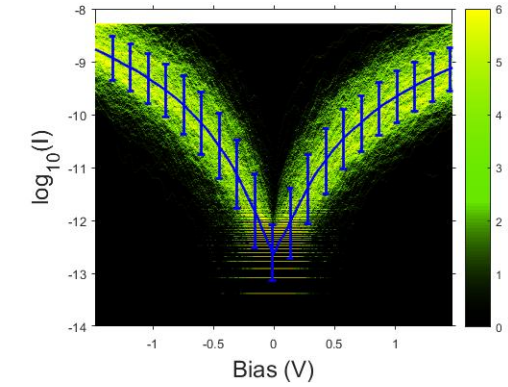

Bottom 2-Ru-C, top 2-Ru-N(dec): low RH

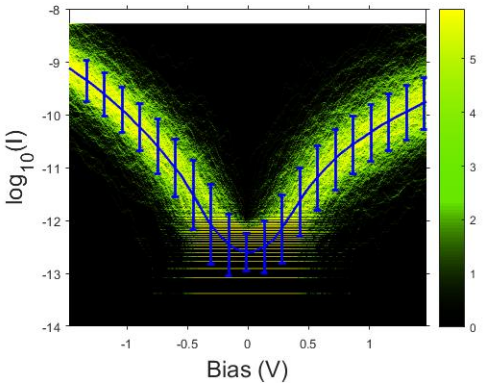

High RH

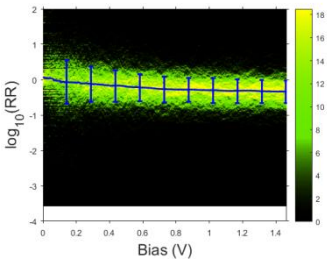

Low RH

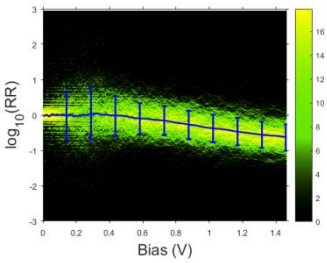

High RH

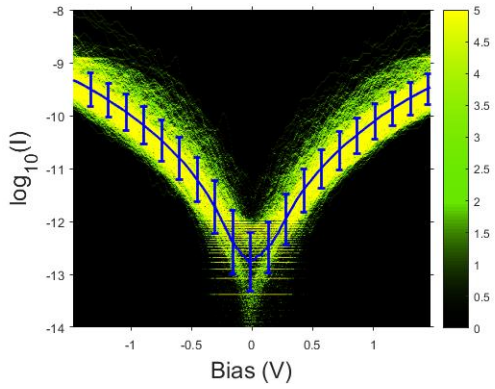

2-Ru-C double layer: low RH

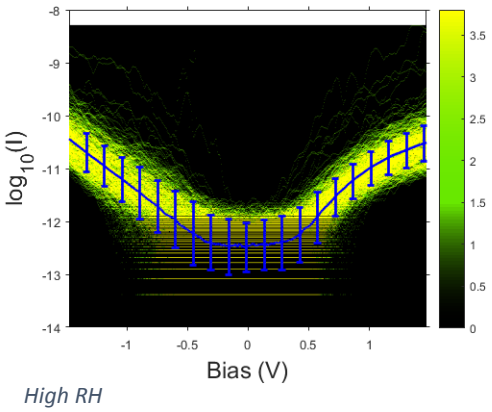

High RH

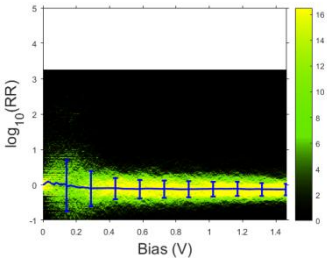

Low RH

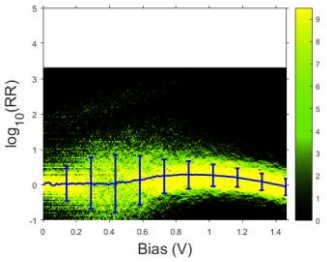

High RH

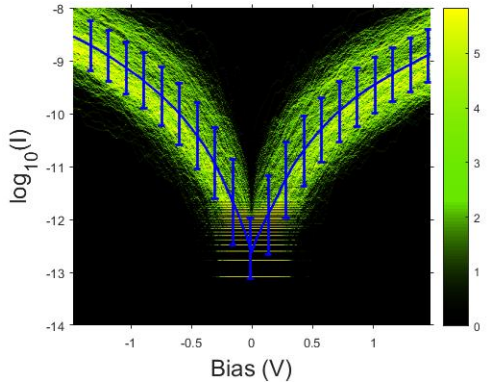

Bottom 2-Ru-C, top 1-Ru-Py: low RH

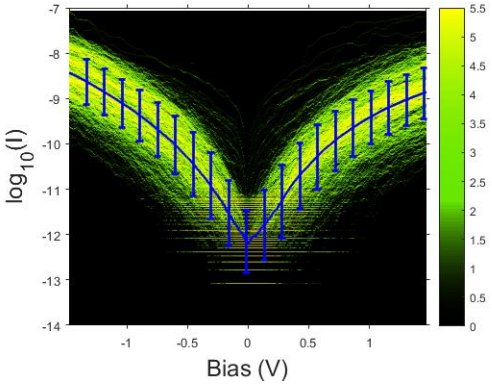

High RH

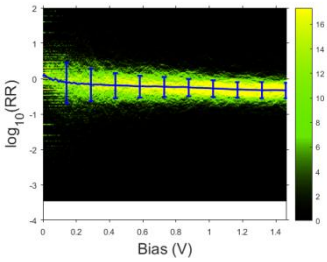

Low RH

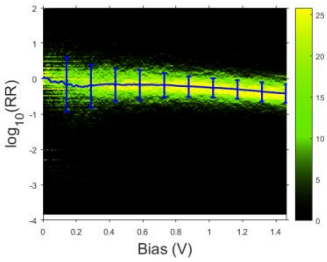

High RH

1-Ru-N multilayers (n=1-3)

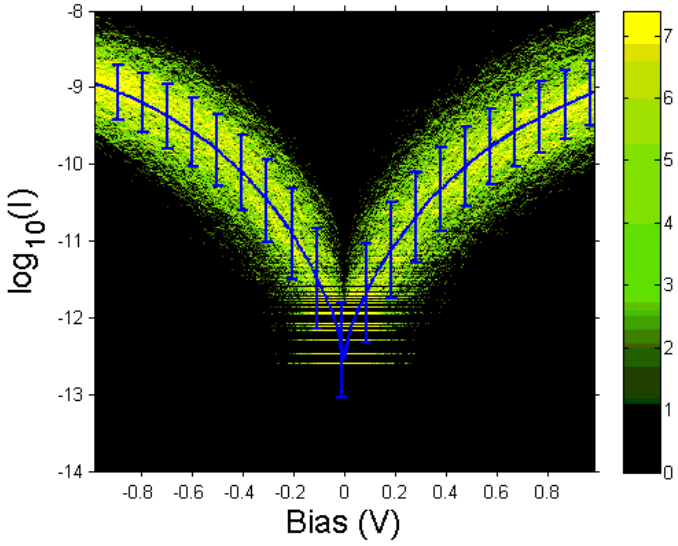

Monolayer 1-Ru-N: low RH

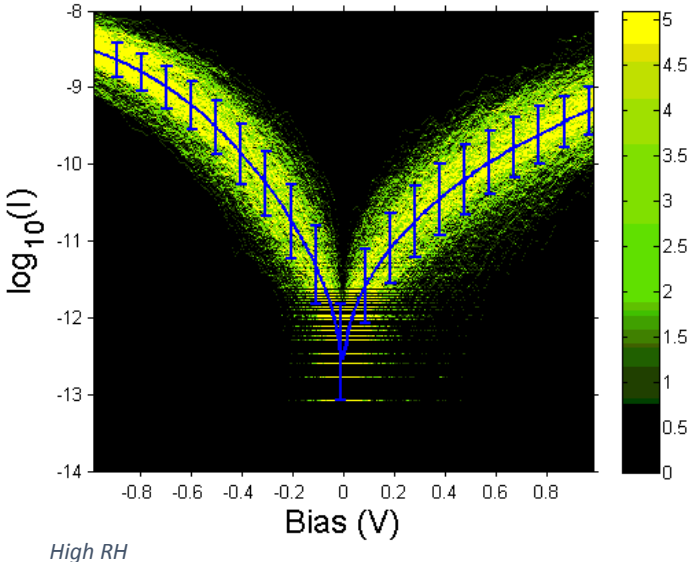

High RH

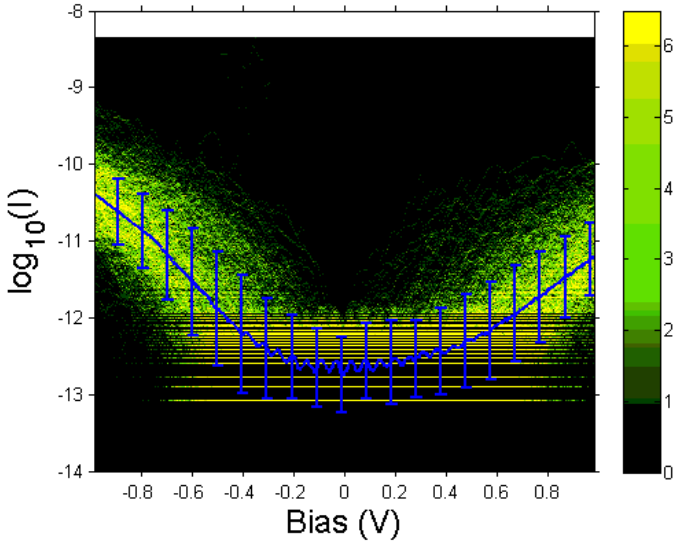

Double layer 1-Ru-N: low RH

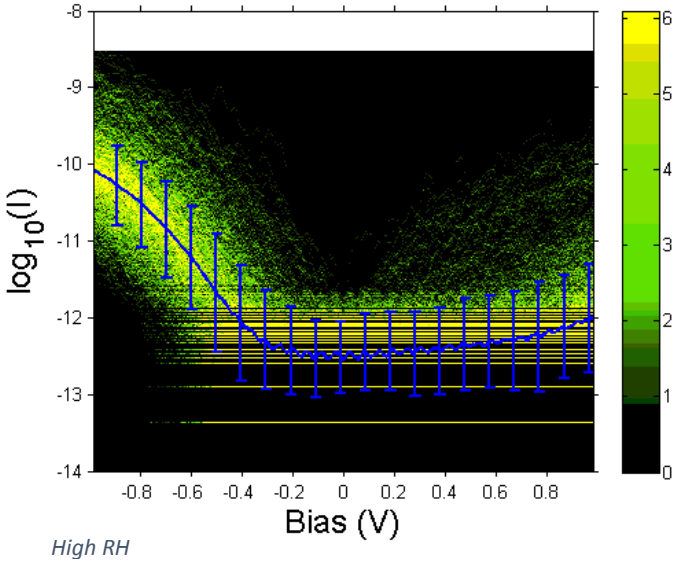

High RH

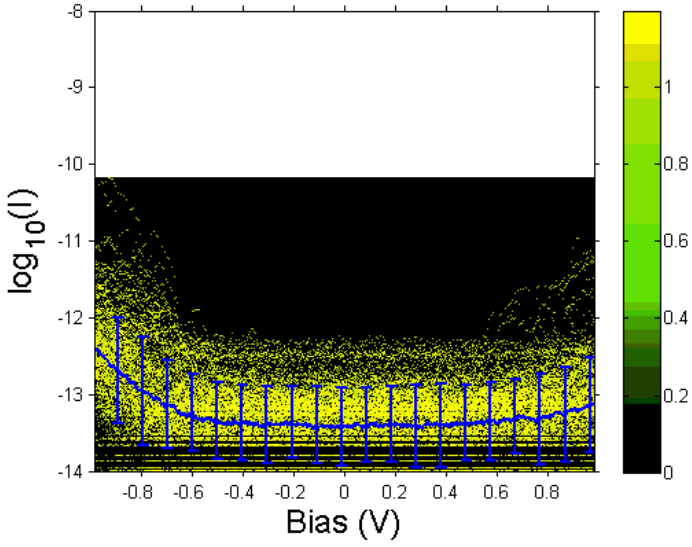

Trilayer 1-Ru-N: low RH

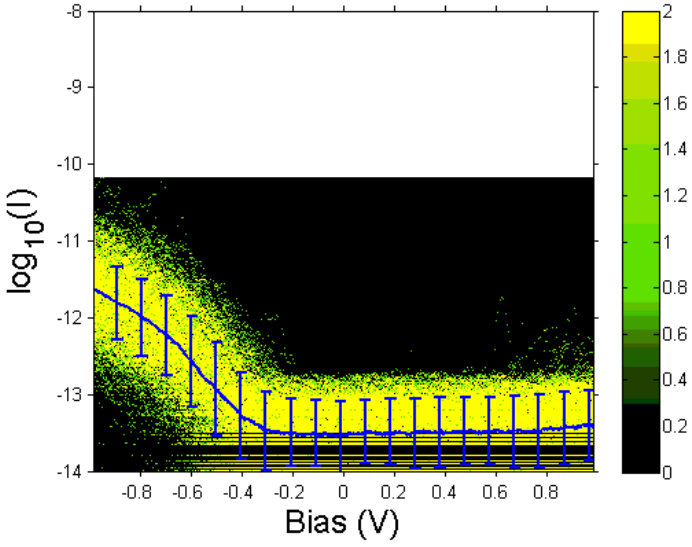

High RH

References

[1] Aviram, Arieh & Mark A. Ratner (1974). Molecular Rectifiers, *Chemical Physics Letters*, **29**, 277-283

[2] Elbing, M. et al. (2005). A single-molecule diode. *Proc Natl Acad Sci* **USA 102(25)**, 8815–8820

[3] Lörtscher, E. (2013). Wiring molecules into circuits, *Nature Nanotechnology*, **8:** 381–384

[4] Guédon, C. M. (2012) Molecular Charge Transport: Relating Orbital Structures to the Conductance Properties, *Gildeprint Drukkerijen*

[5] Perrin, M. (2015). Charge Transport Through Single-Molecule Junctions., *BOXPress*.

[6] Datta, S. (2005). Quantum Transport: Atom to Transistor*, Cambridge University Press*

[7] Capozzi, B. et al. (2015). Single-molecule diodes with high rectification ratios through environmental control, *Nature Nanotechnology*, **10(6):** 522-528

[8] Atesci H., Kaliginedi V. et al. (2016). Switchable rectification of ruthenium-complex molecular junctions, *unpublished paper*

[9] Zotti, L.A. et al. (2010). Revealing the Role of Anchoring Groups in the Electrical Conduction Through Single-Molecule Junctions*, Small,***6(14):** 1529-1535

[10] Pradhan, B. and Das, S. (2008). Role of New Bis(2,2′-bipyridyl)(triazolopyridyl)ruthenium(II) Complex in the Organic Bistable Memory Application, *Chem. Mater*, **20**: 1209-1211

[11] Wu, Y.Z. Length-Dependent Conductance of Conjugated Molecular Junctions, *S1951319*

[12] Wang, G. et al. (2011). Electrical transport characteristics through molecular layers, *Journal of Materials Chemistry*, **21(45):** 18117-18136

[13] Rigaut, S. (2013). Metal Complexes in Molecular Junctions, *Dalton Transactions, Royal Society of Chemistry*, **42**: 15859-15863

[14] Lee, J., et al. (2009). Molecular Monolayer Nonvolatile Memory with Tunable Molecules, *Angewandte Chemie*, **121**: 8653–8656

[15] Mahapatro, A. K., Ying,J., Ren, T. and Janes, D.B. (2008). Electronic transport through ruthenium-based redox-active molecules in metal−molecule−metal nanogap junctions, *Nano Lett*., **8:** 2131

[16] Schwarz, F., Kastlunger, G. et al. (2016). Field-induced conductance switching by charge-state alternation in organometallic single-molecule junctions, *Nature Nanotechnology*, **11:** 170-176

[17] BongSoo, K., Beebe J. M. et al. (2007). Temperature and Length Dependence of Charge Transport in Redox-Active Molecular Wires Incorporating Ruthenium(II) Bis(σ-arylacetylide) Complexes, *J. Phys. Chem. C*, **111 (20)**: 7521–7526

[18] Hines, T., Diez-Perez, I. et al. (2010). Transition from tunneling to hopping in single molecular junctions by measuring length and temperature dependence, *J. Am. Chem. Soc*., **132**: 11658-11664

[19] Putvinski, T.M. et al (1990). Self-Assembly of Organic Multilayers with Polar Order Using Zirconium Phosphate Bonding between Layers, *Langmuir*, **6:** 1567-1571

Images

[a] http://www.ferroic.mat.ethz.ch/research/our-laboratories/atomic-force-microscope.html